

國立交通大學

電機學院光電顯示科技產業研發碩士班

碩士論文

新型雙螢幕立體影像顯示器之
光學系統設計製作與應用



Design, Fabrication and Application of Optical System
for Novel 3D Double-screen Display

研究生：賴郡弘

指導教授：謝漢萍 教授

中華民國九十六年一月

新型雙螢幕立體影像顯示器之
光學系統設計製作與應用

Design, Fabrication and Application of Optical System
for Novel 3D Double-screen Display

研究生：賴郡弘

Student: Chun-Hung Lai

指導教授：謝漢萍

Advisor: Dr. Han-Ping D. Shieh



國立交通大學
電機學院光電顯示科技產業研發碩士班
碩士論文

A Thesis

Submitted to College of Electrical and Computer Engineering

National Chiao Tung University

in partial Fulfillment of the Requirements

for the Degree of

Master

in

Industrial Technology R & D Master Program on

Photonics and Display Technologies

January 2007

HsinChu, Taiwan, Republic of China.

中華民國九十六年一月

新型雙螢幕立體影像顯示器之 光學系統設計製作與應用

研究生:賴郡弘

指導教授:謝漢萍

國立交通大學 電機學院

摘要

隨著知識經濟時代的來臨，視覺影像處理及表達方式也越來越多元化，而現今的顯示器技術卻無法在單一畫面中完整及真實的呈現所有資訊。為了解決螢幕空間不足，並獲得虛擬實境的效果，本論文提出一新型雙螢幕 3D 顯示器來同時獲得兩個全螢幕大小的立體畫面。

根據菲涅耳定律，本光學系統設計能更精簡的只利用平面鏡和柱狀透鏡組成，以產生 3D 和雙螢幕的效果。而此微光學結構是以直寫式準分子雷射加工系統製作，相較於傳統黃光製程方法，如：灰階光罩及光阻熱熔等製程技術，能更精密的控制元件之光學品質、有效的減少其製程步驟與降低成本，以利大量生產。再藉由優化柱狀透鏡的曲率、尺寸及焦距後，串音效應可以有效的消除，進而達到廣視角的效果。因此，在導入影像處理技術於系統中，觀眾可以分別於上下螢幕中同時欣賞到兩個不同的立體影像。綜合實驗成果，本研究所提出的光學系統具高度潛力來轉換一般顯示器為新型雙螢幕 3D 顯示器，並更實際地被應用於顯示器產業。

Design, Fabrication and Application of Optical System for Novel 3D Double-screen Display

Student: Chun-Hung Lai

Advisor: Dr. Han-Ping D.Shieh

National Chiao Tung University

Abstract

3D technique is essential for achieving high realistic feelings of images in current displays. In this new era, things are more and more complicated. An ordinary display does not have characteristics to show all the specific information in a single screen. In order to solve the issues of insufficient screen space and also provide the realistic images, a novel 3D double-screen display is proposed to generate dual full-sized 3D images simultaneously.

According to Snell's Law, the proposed optical system for generating 3D and double-screen images is designed based on a single panel with only two additional components required: a planar mirror and a lenticular-lens based micro-optical structure. By modifying the lenticular-lens' shape, size and position, the crosstalk issues were eliminated and the larger viewing angles were obtained. In addition, the micro-optical structure was fabricated by Excimer Laser Micromachining System without gray-scale mask. Based on its direct writing fabrication process, the shorter process time and the simpler steps are the advantages of producing huge amounts of precise functioning layers in economy and efficient. Moreover, the studies of implementing digital image processing and combining hardware components in the ordinary flat panel display provided viewers of two 3D images at top and bottom screens respectively and simultaneously. The low cost and simple converting technique of the proposed optical system for 3D double-screen displays, thus, promote the possibility of applications in display industry.

Acknowledgement

In my two-year graduate life, I am especially grateful to Professor Han-Ping D. Shieh, who gave me many valuable advices and abundant resources. He never told me what the manner to my research should be, but his attitude towards works is just exemplariness to me. Besides, I also appreciate Professor Yi-Pai Bounds Huang and Dr. Jung-An Cheng, who gave me many useful feedbacks and suggestions to reap no little benefits.

Besides, my classmates, Ming-Lung Chen, Sue-Ping Yan, Chia-Feng Yang, Chien-Jui Huang, Chien-Wen Lin, Young-Jhih Chen, Ming-Jing Chieh and Wan-Ling Yang etc., have accompanied me during these days and brought me many joys. Those younger classmates, Yu-Shing Chuang, Young-Jhih Chen, Cheng-Yumr Liao, Kun-Yuen Lin, Jen-Chieh Hsieh, Wuan-Zheng Yi and Gwo-Jenn Wang etc., and those senior classmates, An-Chi Angel Wei, Chun-Ho Chen, Chi-Huang Lionel Lee, Jen-Yu Ray Fang, Chiao-Shun Patric Chuang, Yu-Kuo Cheng, Po-Ru Paul Yang, Fang-Cheng Lin and Wallen Mphepo etc., all helped me a lot in my life. Certainly, the beautiful, kind and sweet secretaries, particularly Ms. Vivian Ni, also aided me a lot in administration affairs.

I also heartfully acknowledge Instrument Technology Research Center (ITRC) for providing the fabrication materials and equipments, and appreciate Mr. Hui-Hsiung Frank Lin, Chih-Sheng Yu and Dr. Jyh-Rou Sze etc. for the technical support and valuable discussion. Their encouragement greatly motivates the birth of this thesis.

Finally, I have to extremely owe my most lofty esteem to my parents, my lovely younger brother and sister, who always support me silently. What I may accomplish today is inevitably cultivated by what they devoted to me.

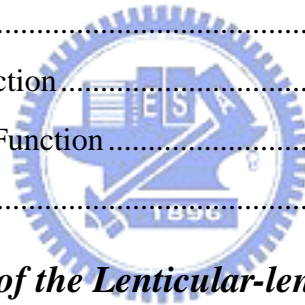
Without these people, this thesis would never have seen the light of day.

Chun-Hung Lai in January, 2007

Table of Contents

摘要.....	i
Abstract.....	ii
Acknowledgement	iii
Table of Contents	iv
Figure Captions	vii
List of Tables	xi
Chapter 1 Introduction	1
1.1 Development of Electronic Displays	1
1.2 Desirous of Future Displays.....	2
1.3 Motivation and Objective of this Thesis	3
1.4 Organization of this Thesis	4
Chapter 2 Principles of Proposed 3D Double-screen Display	5
2.1 Overview	5
2.2 Principles of 3D Vision	6
2.3 3D Display Technologies	8
2.3.1 Stereoscopic Displays	8
2.3.2 Auto-stereoscopic Displays.....	8
2.3.3 Comparisons of 3D Methods	13
2.4 Dual-view Display Technologies	15
2.5 Design of Single Panel 3D Double-screen Display	17
2.5.1 Model Adopted	18
2.5.2 Functioning Principles	19
2.6 Applied Fields of 3D Double-screen Display	20
2.7 Summary	21
Chapter 3 Design of Lenticular-lens-based Micro-optical Structure for 3D and Double-screen Functions	23
3.1 Introduction.....	23

3.2 Optical Design of Micro-optical Structure.....	23
3.2.1 Lens Design	24
3.2.2 Functions Design	27
3.2.3 Structure Design	27
3.3 Image Quality.....	29
3.3.1 Crosstalk Issue	29
3.3.2 Determination of Acceptable Viewing Angle Range	30
3.4 Optimizing Viewing Performance	31
3.4.1 Material Refraction Index Effect	32
3.4.2 Substrate Thickness Effect.....	33
3.4.3 Lens Radius Effect.....	34
3.5 Simulations	36
3.6 Simulated Results and Discussions.....	36
3.6.1 3D Function	36
3.6.2 Double-screen Function.....	38
3.6.3 3D Double-screen Function.....	40
3.7 Summary	41



Chapter 4 *Fabrication of the Lenticular-lens-based Micro-optical Structure by Excimer Laser Micromachining System*.....43

4.1 Introduction.....	43
4.2 Fabrication Principle	44
4.2.1 Fabrication Process	44
4.2.2 Excimer Laser Micromachining System.....	46
4.2.3 Micromachining Technique	47
4.3 Fabrication Stability and Lens Quality	49
4.3.1 Energy Stability.....	49
4.3.2 Lens Radius with Laser Energy	50
4.3.3 Lens Radius with Laser Penetration Rate	51
4.3.4 Lens Radius with Stage Feeding Rate	52
4.4 Fabrication Tolerances	53
4.4.1 Dual Curvatures Effect	53

4.4.2 Lens Gap Effect	54
4.5 Experiments	55
4.6 Experimental Results and Discussions	59
4.6.1 Lens Radius.....	59
4.6.2 Viewing Angle for 3D and Double-screen Functions.....	61
4.7 Summary	63
Chapter 5 Mechanism of Converting an Ordinary Flat Panel Display to 3D Double-screen Display	64
5.1 Introduction.....	64
5.2 Algorithm of Digital Image Process	64
5.3 Alignment of Micro-optical Structure.....	67
5.3.1 Aliasing	68
5.3.2 Moiré Patterns.....	69
5.4 Experimental Results	70
5.5 Discussions	74
5.6 Summary	75
Chapter 6 Conclusions and Future Works	76
6.1 Conclusions.....	76
6.2 Features	77
6.3 Future Works.....	77
Reference.....	79



Figure Captions

Fig. 1-1. Historical development of the electronic displays. 1

Fig. 1-2. The multi-screen display. 2

Fig. 2-1. Depth clues and display factors..... 7

Fig. 2-2. Examples of 3D methods: (a) volumetric 3D display system with rasterization hardware; (b) a solid-state multi-planar volumetric display; (c) DSHARP - a wide screen multi-projector display; (d) color images with the MIT holographic video display; (e) the concept of integral imaging; (f) the principles of stereo pair type: spatial-multiplexed and time-multiplexed displays. 12

Fig. 2-3. The stereo type of 3D display (a) parallax barrier and (b) lenticular-lens. ... 12

Fig. 2-4. 3D mobile display based on sequentially switching backlight. 13

Fig. 2-5. 3D mobile display based on dual directional stacked lightguides. 13

Fig. 2-6. Concept of a) single-view and b) dual-view display, and c) single-view and d) dual-view images. 15

Fig. 2-7. The stereo type of dual-view display (a) parallax barrier and (b) lenticular-screen..... 16

Fig. 2-8. Concept of the proposed 3D double screens display system. 18

Fig. 2-9. Configuration of the top screen with micro-optical structure. 18

Fig. 2-10. Schematic of the micro-optical structure. 20

Fig. 3-1. Schematic of lenticular-lens based 3D display. 26

Fig. 3-2. Lens pitch of (a) 594 μm for 3D and (b) 1188 μm for double-screen image. 27

Fig. 3-3. The structure layout of lenticular-lenses with color filter's pixels (a) in portrait and (b) in landscape with respected theoretical images of (c) portrait for 3D and (d) landscape for double screens. 28

Fig. 3-4. Definition of crosstalk as shown in circle: a) light-spot and b) light-leakage. 30

Fig. 3-5. The range of acceptable viewing angles after considering the crosstalk. 31

Fig. 3-6. Results of right eye's 3D or right direction double-screen images with varies material refraction index: (a) $n=3$, (b) $n=2$, (c) $n=1.7$, (d) $n=1.5$ and (e) $n=1.3$.	32
Fig. 3-7. Relationship between the lenticular-lens radius and viewing angles for (a) general case, (b) 3D function and (c) double-screen function.	35
Fig. 3-8. Schematic diagram of viewing angles at near and further viewing positions.	37
Fig. 3-9. Angular distribution of proposed 3D function for (a) left and (b) right eye's image, and (c) and (d) are their respected cross-section intensity distribution in horizontal orientation.	38
Fig. 3-10. Angular distribution of proposed double-screen function for (a) bottom and (b) top direction image, and (c) and (d) are their respected cross-section intensity distribution in vertical orientation.	39
Fig. 3-11. Schematic diagram of acceptable viewing-angles for top and bottom screens.	40
Fig. 3-12. Angular distributions of the proposed 3D double-screen display for (a) left and (b) right eye's images of top screen; (c) left and (d) right eye's images of bottom screen.	41
Fig. 4-1. Detailed fabrication processes of general lithography technology.	45
Fig. 4-2. Detailed fabrication processes of excimer laser micromachining technology.	46
Fig. 4-3. Schematic diagram of excimer laser micromachining system.	47
Fig. 4-4. Prism structure fabricated by scanning with a contour mask.	48
Fig. 4-5. Schematic of contour mask for fabricating lenticular-lenses.	48
Fig. 4-6. Excimer laser energy for 4 weeks continuously.	50
Fig. 4-7. Deviation of laser shot for each week.	50
Fig. 4-8. Lens radius with laser energy.	51
Fig. 4-9. Lens radius with laser penetration rate.	52
Fig. 4-10. Lens radius with stage feeding rate.	53
Fig. 4-11. Schematics of (a) singular curvature and (b) dual curvatures lens structures.	

.....	54
Fig. 4-12. Simulated results of half lens with radius of 150 um and another half with radius (a) 200 um, (b) 150 um, (c) 140 um and (d) 100 um.	54
Fig. 4-13. Schematics of lens structures with (a) no gap and (b) gaps, and their respected simulated results.	55
Fig. 4-14. Appearances of Excitech7000.....	56
Fig. 4-15. Outlook of a set of lenticular-lenses to be fabricated.....	57
Fig. 4-16. Appearances of Zygo’s optical interferometer.	58
Fig. 4-17. Appearances of ELDIM EZContrast 160 measurement system.	58
Fig. 4-18. Photograph of sample fabricated lenticular-lens for double-screen function.	60
Fig. 4-19. Measured results of Zygo’s interferometer.....	60
Fig. 4-20. Angular distributions of simulated results on (a) top screen of double-screen function and (b) right eye of 3D function, and the experimental results on (c) top screen of double-screen function and (d) right eye of 3D function.	62
Fig. 5-1. Concept map of 3D double-screen images algorithm.	65
Fig. 5-2. Real images map of 3D double-screen images algorithm.....	66
Fig. 5-3. The schematic outlook with (a) left and right pixels for 3D function and (b) top and bottom pixels for double-screen function.	66
Fig. 5-4. (a) Right eye [R], (b) left eye [L] and (c) 3D [R+L] images.....	67
Fig. 5-5. (a) Bottom screen [B], (b) top screen [T] and (c) double-screen [B+T] images.	67
Fig. 5-6. Angular distributions of the double-screen function for (a) aligned well, (b) 0.1 mm tolerance and (c) 0.2 mm tolerance with their respective outlooks (d), (e) and (f).....	69
Fig. 5-7. Cause of moiré patterns.....	70
Fig. 5-8. Demonstrated results of (a) image without, 3D images of (b) left eye and (c) right eye, and black & white images of (d) left eye and (e) right eye with attaching micro-optical structure on the panel.....	72

Fig. 5-9. Demonstrated result of the panel with attaching another set of lenticular-lenses (top screen's circle area) for (a) processed images and (b) white & black strips for double-screen function.....73

Fig. 5-10. Demonstrated results of (a) without attaching micro-optical structure's image and with attaching for (b) left and (c) right eye's 3D double-screen images.73



List of Tables

Table 2-1. Comparisons between various 3D displays. 14

Table 2-2. Comparison of displays using lenticular-lens and parallax-barrier. 19

Table 2-3. Possible fields of using 3D double-screen display..... 21

Table 3-1. Comparison of 3D and double-screen functions' parameters. 31

Table 3-2. Substrate thickness with its respected light intensity distributions. 33

Table 3-3. Calculated 3D double-screen display parameters. 36

Table 4-1. Micromachining parameters. 57

Table 4-2. Fabrication targets for the lenticular-lenses arrays. 57

Table 4-3. Fabrication parameters and resultant lenses radii of each trail..... 61



Chapter 1

Introduction

1.1 Development of Electronic Displays

Since the world merged into the information age, there are lots of discoveries and products yield profound impacts on the civilization in many fields, such as entertainment, education, military, and communication. In particular, the electronic display technologies have motivated people to develop more powerful and comfortable display technologies in all fields.

From a century ago, the electronic display technologies have developed with several milestones as shown in Fig. 1-1 [1]. In 1897, K. F. Braun invented the cathode ray tube (CRT) which is the earliest ancestor of the following various kinds of CRT monitors and TVs. The success of the CRT opened the door to the development of flat panel display (FPDs) technology such as liquid crystal displays (LCDs) and plasma display panels (PDPs). They are getting more and more popular after 1990s because they not only provide comparable image quality with CRT but also have compact sizes and low power consumption.

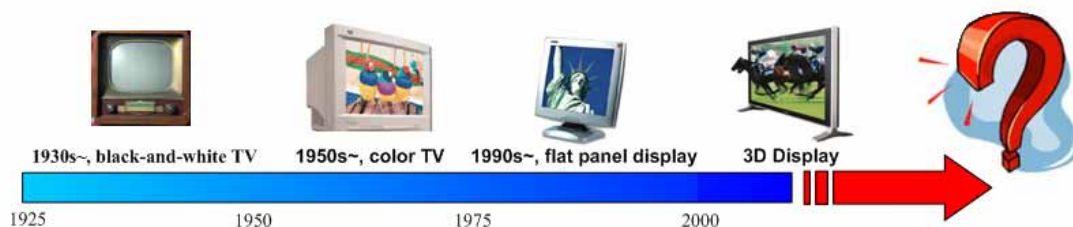


Fig. 1-1. Historical development of the electronic displays.

1.2 Desirous of Future Displays

During these years, significant progress has been made in image qualities and compact instruments, i.e. from black-and-white to color types and bulky to compact sizes. Numerous scenes and information are reproduced and spread by the electronic displays. However, the image qualities which are still not as good as the real vision perceived by human eyes in the real world are concerned. The display performances of the above-mentioned technologies are limited by one viewpoint of the objects. In another word, there is no stereoscopic sense in the display images which are classified as 2D displays.

In this new era, which can be simply called the Age of Knowledge, more and more messages have to be dealt or considered at the same time. Due to the limitation of the screen size, a singular-screen display may not be able to contain all the required information. Therefore, a display having a function to generate multi-screen images, as shown in Fig. 1-2, will be very valuable.

Since the work becomes more and more complicated in this modern world, human beings are desired to have a better quality and more realistic displays to demonstrate diverse information. For getting images closer to the real world, a single-screen 2D display seems more and more inadequate. Therefore, to develop an environment containing natural viewing and practical needs for observers, a display having functions to generate multi-screen 3D images may be the trend in near future.



Fig. 1-2. The multi-screen display.

1.3 Motivation and Objective of this Thesis

New generation personal information and mobile communication systems, such as mobile phone, hand-held personal computer (HPC), digital camera, and game-boy player have progressed rapidly. Limited-sized display screens and unrealistic images are essential for above applications. A display combining 3D and multi-screen functions are of advantageous of those requirements. However, in order to have both functions work on these portable flat panel displays, several combination techniques are needed to be investigated.

The objective of this thesis is to invent a display system that can generate the dual full-screen-sized 3D images simultaneously by a single panel. This study will develop some fundamental knowledge to enlighten the further research on accomplishing a single panel realistic multi-screen display. Therefore, a novel optical system having these functions has to be proposed and can be divided into three sections: design of micro-optical structure, fabrication techniques and application on flat panel displays.

Because the industry is looking for low cost and high return products, we proposed a low-cost micro-optical structure which can be easily laminated onto the top surface of flat panel displays. The micro-optical structure is designed to contain 3D and double-screen functions when pasting on a single panel portable LCDs for yielding diverse information of 3D images. The theories of the micro-optical devices will be studied and developed for optimizing their viewing performance.

Generally, the micro-optical structure requires very complex fabrication process which may result in a very high cost. However, in the study, the economical fabrication technology, such as semiconductor process with Excimer laser

micromachining technology, has to be developed and utilized to reduce the steps of the process and lower the cost. By using these well-developed fabrication processes, the designed structure can be produced economically and reproducibly in large volume, and is an effective means of producing 3D double-screen displays.

After the proposed micro-optical structure was investigated, the next step is to apply the structure on a panel to enhance the possibility of transforming the ordinary flat panel displays to become a 3D double-screen display. In order to apply the optical system on the existing displays, the mechanism of transformation between ordinary displays and 3D double-screen displays needs to be explored. The digital image process on converting the ordinary images to the required inputs for 3D and double-screen functions has to be studied. The alignment technique is also needed to be explored. Consequence, based on these research efforts, a novel 3D double-screen display can be demonstrated and will become more attractive and competitive in the flat panel applications.



1.4 Organization of this Thesis

The thesis is organized as following: The principles of the proposed 3D double-screen display are presented in **Chapter 2**. In **Chapter 3**, design of lenticular-lens-based micro-optical structure for 3D and double-screen functions were invented and simulated. Moreover, manufacturing the lenticular-lens-based micro-optical structure by excimer laser micromaching system will be explored in **Chapter 4**. In **Chapter 5**, the mechanism of applying the optical system in the ordinary flat panel display is presented. The digital image process method and image demonstrations will be also included. Finally, discussions and summaries of this thesis, and recommendations for the future works are given in **Chapter 6**.

Chapter 2

Principles of Proposed 3D Double-screen Display

2.1 Overview

“Can you imagine one is watching a baseball game and searching the baseball players’ data on the internet at the same time?” The answer to this survey will most likely be positive. If there is an additional assumption that both images are viewed in full-screen size and generated from a single panel display, will you still believe the possibility of this statement? I believe the responds will now become disappointed. However, as a novel 3D double-screen display is proposed, the situation of watching full-screen-sized diverse channels from a single panel is no longer impossible.

In order to design a double-screen display with realistic feeling on images, the study will begin with knowing the fundamental principles of 3D vision. After that, various technologies of generating dual-view and 3D images, such as the methods of stereoscopic and auto-stereoscopic types’ displays, will be discussed and compared. The analyzed results will show a better candidate to utilize for further research. Hence, the 3D and double-screen functions will be developed and introduced. The full design concepts of the proposed novel 3D double-screen display system will also be presented.

2.2 Principles of 3D Vision

Three-dimensional information is formed by complex activities in the brain and obtained by the visual system. A lot of related researches have been made in this field [2]. There are several clues to depth perception by the visual sense as shown in Fig. 2-1 [3, 4].

Convergence

Convergence is effective when the distance between eyes and objects is within 20 m. Convergence rapidly loses its influence on the visual system as the distance increases because the convergence angle becomes smaller.

Binocular Parallax

Binocular parallax occurs when there are other objects in front of or in the rear of the object on which the right-left eyes are focused. If the degree of this binocular parallax is sufficiently small, the images are combined and the observer has a clear sensation of depth in front and behind the object. The binocular parallax is valid and precise in distinguishing the depth difference, i.e. the difference in the distance between several objects. It plays the important role in understanding the relative position of objects within 10 m.

Accommodation and Motion Parallax

Accommodation is only effective when the observation distance is no more than 3 m. Depth perception obtained by motion parallax provides important information to depth perception.



Others

Visual information received by one eye is not the same as that through the other eye, but we perceive these data as a single image. Namely, binocular vision which appears to be based on interaction of the right and left images is an important function in the design of a 3D display. Besides, the distance between the pupils of the human eyes is approximately 65 mm which is adopted when considering the viewing conditions.

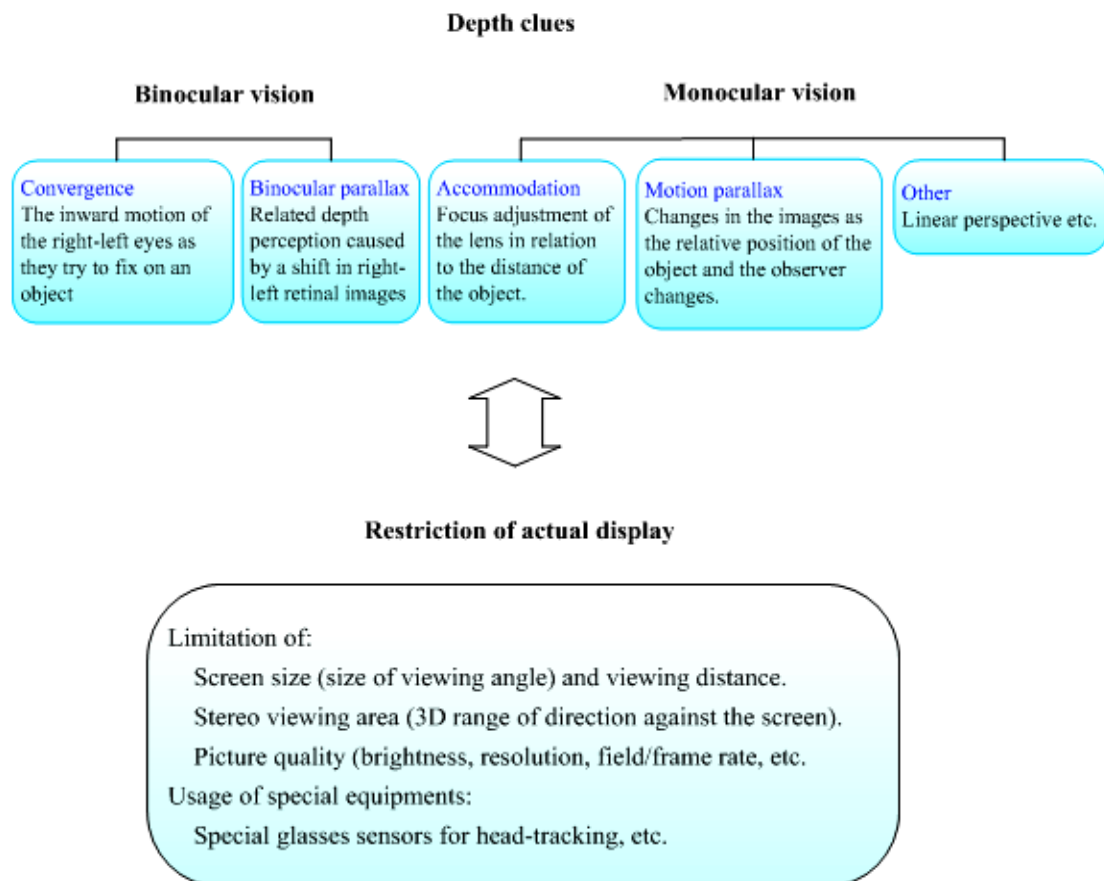


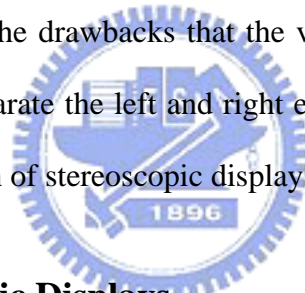
Fig. 2-1. Depth clues and display factors.

2.3 3D Display Technologies

The first of 3D display went back to the early 1800s. However, most applied 3D technologies were proposed after the middle of 20th century. In these few years, the 3D displays have their widespread applications. Generally speaking, the 3D displays can be divided into stereoscopic displays and auto-stereoscopic displays.

2.3.1 Stereoscopic Displays

Stereoscopic displays are needed to wear a device, such as polarized glasses, which ensures the left and right eye's views are received by the correct eye. Many stereoscopic displays have been proposed [5, 6]. Most of them have widely used in many fields but suffer from the drawbacks that the viewer have to wear, or be very close to, some devices to separate the left and right eye's views. Those requirements limit the widespread attraction of stereoscopic displays as personal displays.



2.3.2 Auto-stereoscopic Displays

Auto-stereoscopic displays do not require the user to wear any device to separate the left and right views and instead send them directly to the correct eye. This removes a crucial obstacle to the appealing of 3D display.

Various auto-stereoscopic technologies have been proposed. The principles of several technologies [7] are discussed in the following.

Volumetric type

There are many kinds of technologies to form the volumetric type display. The common point is to produce the object in the real space. One is to draw 3D profiles on a

scattering medium with a scattering laser beam [8], as shown in Fig. 2-2(a). Another is to project or scan layered images on a spatial designed screen to create a volumetric image profile [9, 10], as shown in Fig. 2-2(b). The other is to induce psychological effects with use of a super-large image projection screen [11], as shown in Fig. 2-2(c).

Holography

Holography is utilized the laser beam to form the illumination beam and reference beam. Thereafter, the interference fringes can be displayed by the superposition of rays from each object point [12], as shown in Fig. 2-2(d).

Integral imaging

Integral imaging [13, 14] is composed of a micro-lens array, the pickup device, and the display device. By means of micro-lens array, the pickup device can pick up several images with the different angles. By combining these pick up images, the 3D images can be revealed, as shown in Fig. 2-2(e).

Stereo pair

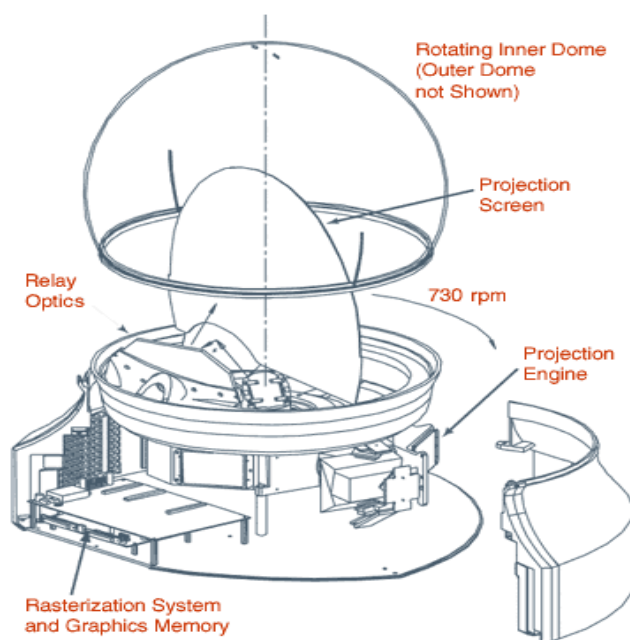
The stereo pair type is including spatial-multiplexed and time-multiplexed display. Both of them require viewing zone forming optics to send the stereo pairs' images to the correct eye. The viewing zone is a region where the viewers can see the whole images displayed on the screen. There are two viewing zones to match each eye, than forming a complete 3D vision. In order to form the 3D perception, each display system is needed a specific optical power. The spatial-multiplexed type displays show the stereo pairs' images at the same time, and the time-multiplexed type displays have the stereo pairs' images sequentially, as shown in Fig. 2-2(f).

For the spatial-multiplexed method, the well-known examples are the flat panel with a lenticular screen [15] or a parallax barrier [16, 17], as shown in Fig. 2-3. The concept of using the lenticular screen or the parallax barrier is to separate the images displayed on the panel to form the parallax images. After the parallax images received by human eyes, the brain will reconstruct them to form 3D images.

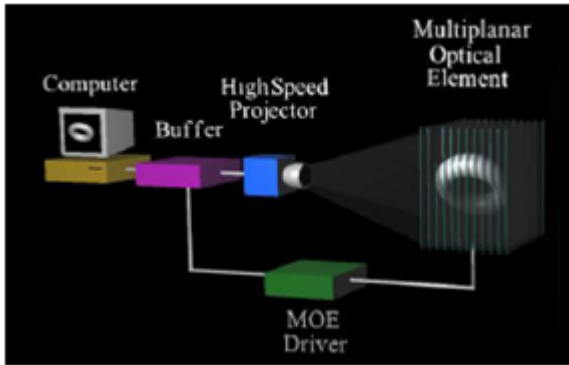
For the time-multiplexed method, its development was restricted in early periods because the fast response time display was not available. During these few years, there are some designs for time-multiplexed 3D display proposed, such as K. W. Chien's, as shown in Fig. 2-4 [18], and Y. M. Chu's, as shown in Fig. 2-5 [19]. The idea of the design is that the parallax images are formed by sequentially switching backlight with focusing foil or the dual directional backlight system. The lightguides provide with right or left eye's light sources to each eye respectively. By switching the light sources sequentially, the stereo pairs' images can be perceived by eyes one after another, then form the 3D image.



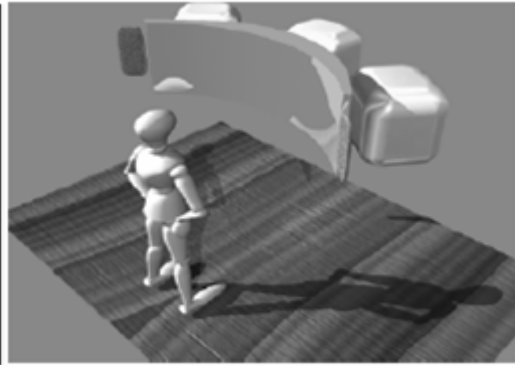
Method (a)



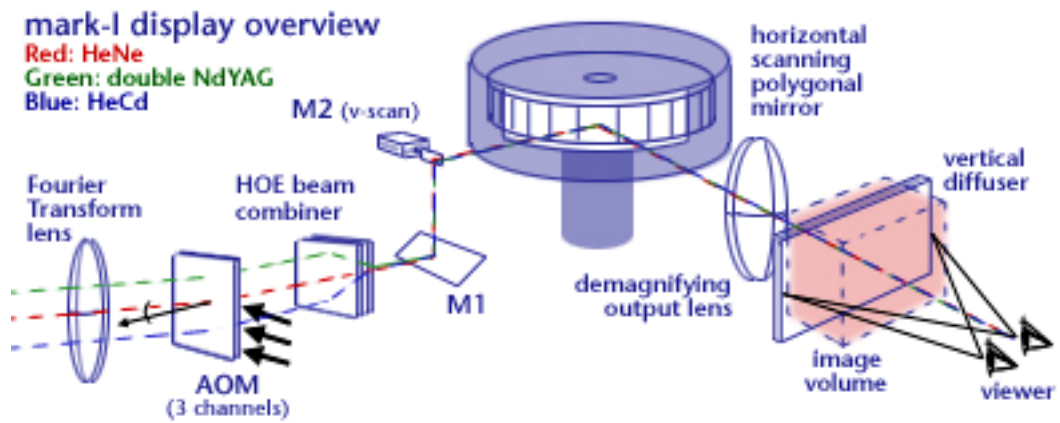
Method (b)



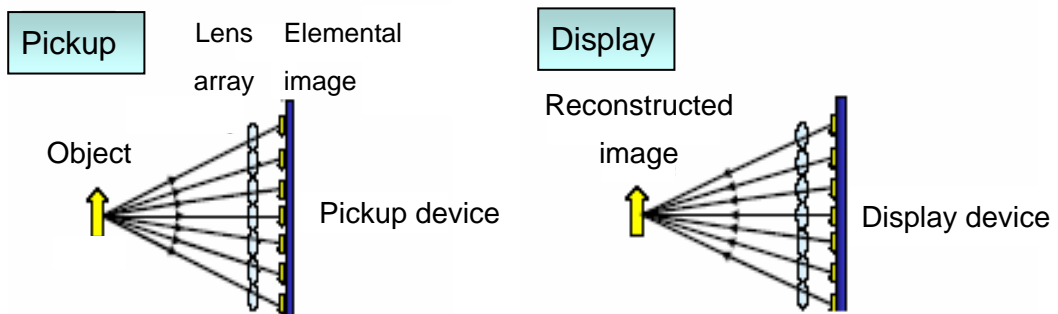
Method (c)



Method (d)



Method (e)



Method (f)

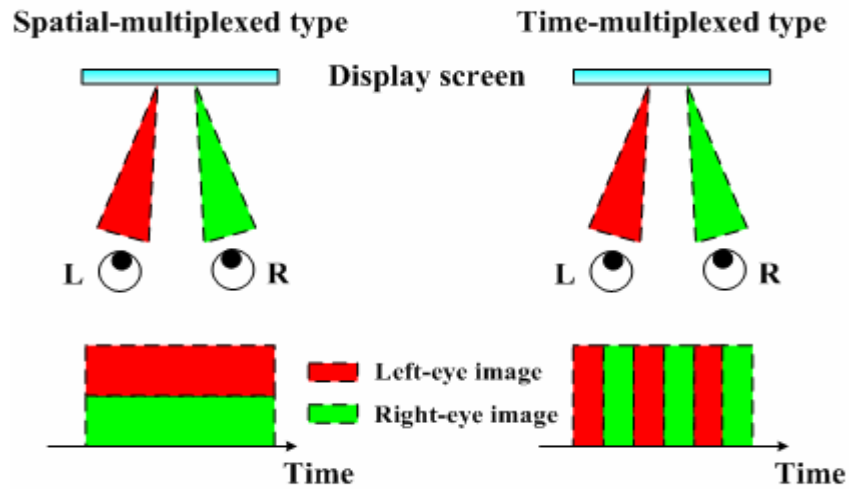


Fig. 2-2. Examples of 3D methods: (a) volumetric 3D display system with rasterization hardware; (b) a solid-state multi-planar volumetric display; (c) DSHARP - a wide screen multi-projector display; (d) color images with the MIT holographic video display; (e) the concept of integral imaging; (f) the principles of stereo pair type: spatial-multiplexed and time-multiplexed displays.

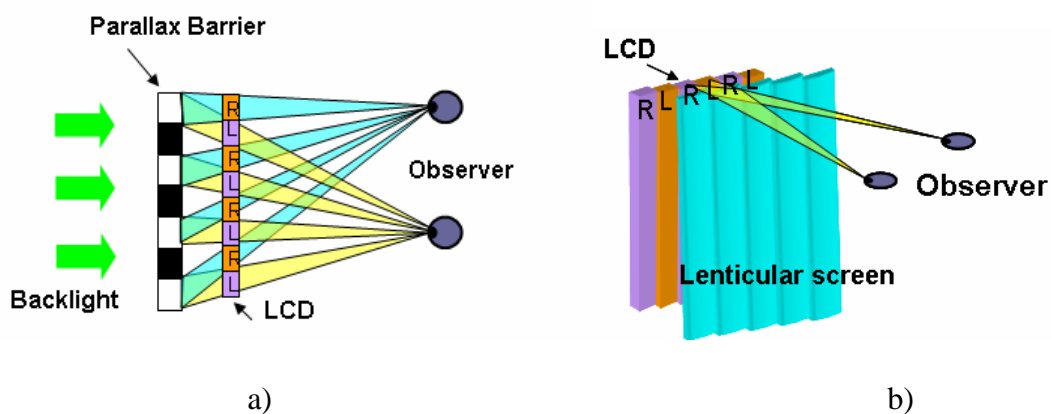


Fig. 2-3. The stereo type of 3D display (a) parallax barrier and (b) lenticular-lens.

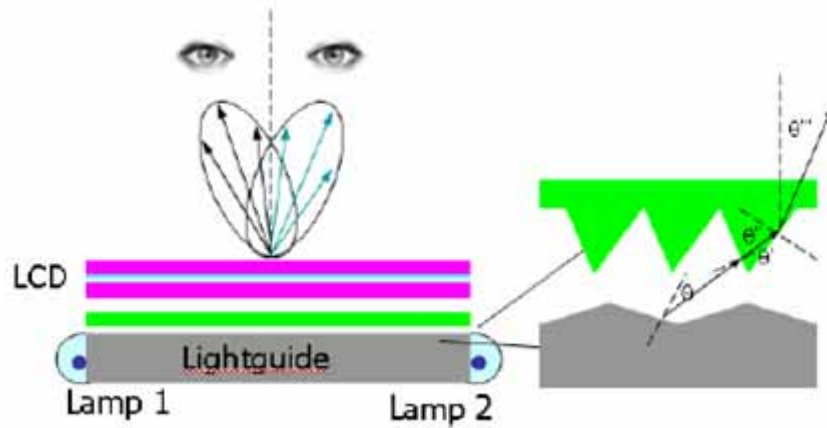


Fig. 2-4. 3D mobile display based on sequentially switching backlight.

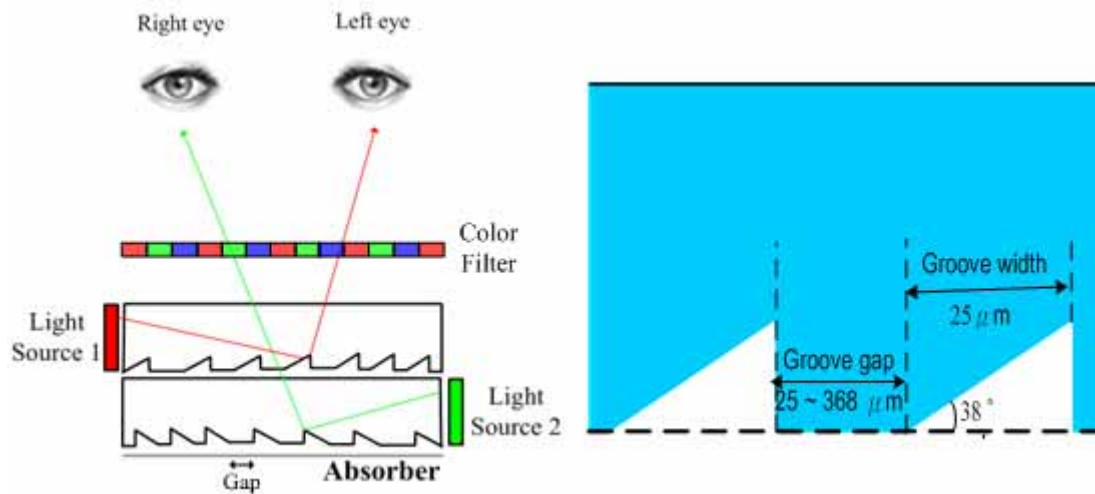


Fig. 2-5. 3D mobile display based on dual directional stacked lightguides.

2.3.3 Comparisons of 3D Methods

By summarizing various 3D display technologies introduced, there are two ways to generate the sense of depth. The first one is to simulate the objects in the real space, as mentioned by methods (a) to (d). The other is to directly send pairs of parallax images to each eye respectively, as mentioned by methods (e) and (f). These 3D displays can yield acceptable 3D images, but most of them can not provide the solutions to our design completely.

According to the 3D image qualities, system size and cost, each 3D method has their advantages and disadvantages as shown in Table 2-1[20]. The major drawback of stereoscopic display is needed to wear a device. Moreover, the volumetric display often has the drawbacks of bulky and 3D effect limitation. Furthermore, the holographic display has the poor feasibility due to the requirement of ultrahigh technical support. The concept of integral imaging is similar to the stereo pair but has the drawback of low image resolution. The overall evaluations of the stereo pair type are the most appealing, not only has compatibility with the current 2D display technology but also maintain the image qualities. Besides, the stereo pairs display has higher feasibility than the other 3D methods. Therefore, the stereo pair display is a better candidate to be widely applied for most of available auto-stereoscopic displays.

Table 2-1. Comparisons between various 3D displays.

	<u>Auto-stereoscopic</u>			
	<u>Stereoscopic</u>	<u>Volumetric</u>	<u>Holographic</u>	<u>Stereo Pair</u>
Natural depth	✕-△	✕-△	△-○	△-○
Viewer comfort	○	✕-△	△-○	△-○
Group viewing	○	○	○	△-○
Compact size	○	✕-△	✕	△-○
Moderate price	○	✕-△	✕	○
Compatibility: 2D/3D	○	△-○	✕-△	○
No degrade image quality	○	△-○	△	○

○: Possible △: Some cases possible ✕: Impossible

The stereo pair displays contain two methods, spatial-multiplexed and time-multiplexed. Both of them are commonly chosen. However, the time-multiplexed type displays have some issues on alignment and response time in the early stage. In 2003, K. W. Chien's designs [18] still had major defect on inadequate light efficiency which resulted from the grooves of the lightguide which

were too flat to guide light effectively. Then, Y. M. Chu provided the solution in her design [19], but moiré pattern is formed by the periods of color filter and two stacked lightguides. Even in Y. C. Yeh's design [21], moiré pattern can not be eliminated completely. Therefore, due to the heavy uncertainties of time-multiplexed method, we choose to utilize the other more mature method, spatial-multiplexed.

2.4 Dual-view Display Technologies

In 2005, a new type of display which could perform dual full sized images simultaneously has been announced [27]. The users at right side of the panel could enjoy the TV game while the other observers at left side were watching the video content such as a movie or a TV broadcast. The differences of single-view and dual-view displays are shown in Fig. 2-6.

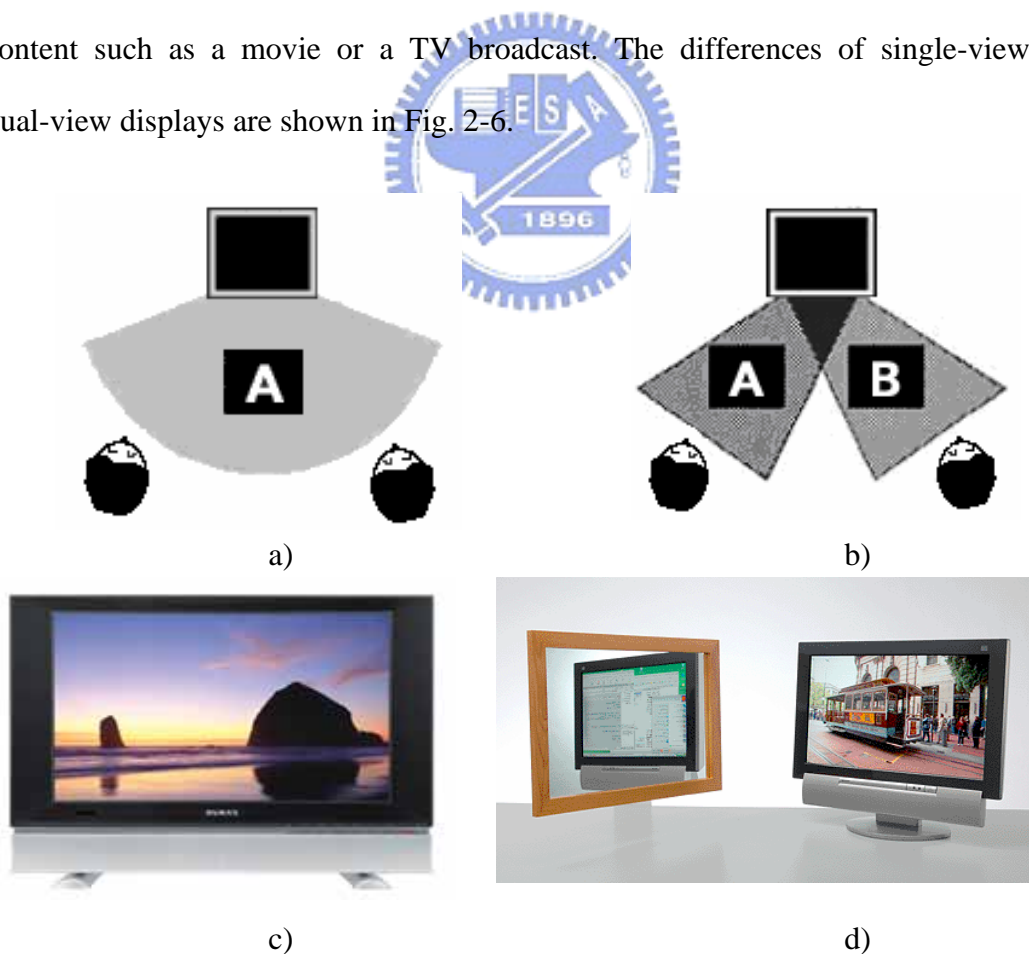


Fig. 2-6. Concept of a) single-view and b) dual-view display, and c) single-view and d) dual-view images.

These dual-view TVs were basically designed from extending the 3D display technologies. The stereo pair type spatial-multiplex systems including parallax barrier and lenticular-screen are the general methods as shown in Fig. 2-7. The first prototype dual-view display is using parallax barrier. Superimposing the parallax barrier as the external micro-optical layer on an ordinary TFT-LCD as their two-way viewing-angle LCD was proposed [27]. The observers standing at left or right positions can view the left or right side images, respectively. The opposite images are blocked by the parallax barrier. Because parallax barrier is designed to block certain areas of images, the light efficiency becomes half of the ordinary. Therefore, some research groups are investigating on utilizing the lenticular-screen [28]. The left and right side images are re-directed by the lenticular-screen to left side and right sides, respectively. This will enable the viewers standing at each side to receive different visual information.

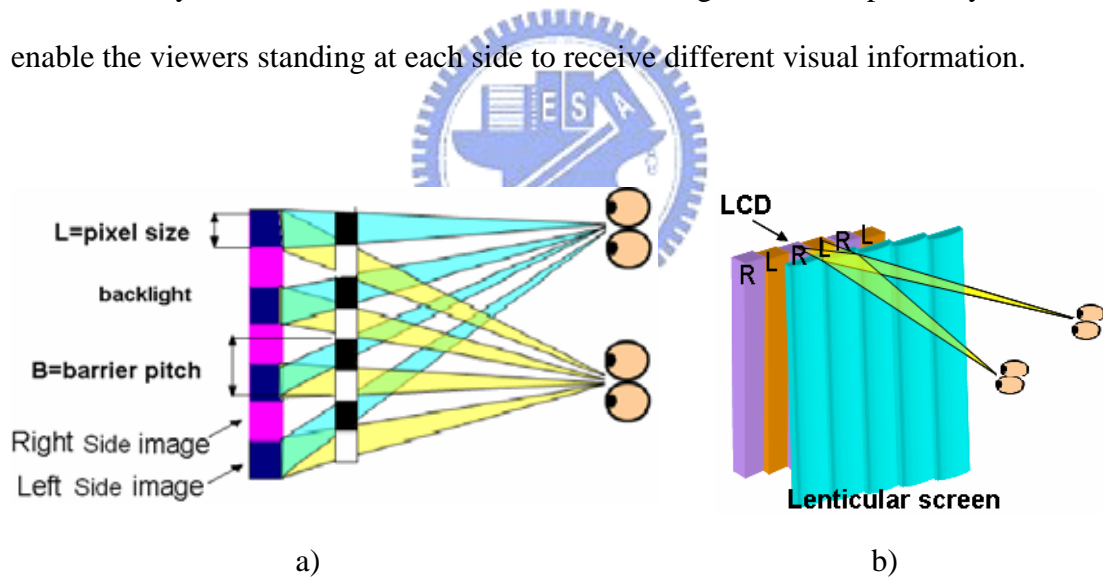


Fig. 2-7. The stereo type of dual-view display (a) parallax barrier and (b) lenticular-screen.

2.5 Design of Single Panel 3D Double-screen Display

Among various display technologies developed to visualize 3D and dual-view images, the lenticular-lens based spatial-multiplexed method has been selected in our research to enjoy its benefits of high brightness and availability of generating multiple views [21, 22]. In deed, the extension of concept on generating multiple views shows a set of the lenticular-lenses can split and guide the images to the specific directions and to perform either 3D or dual-view function by the proper lens design [23].

The difference between dual-view and double-screen functions is the amount of images perceived by viewers. By utilizing dual-view function in the display, observers standing at left and right of display can see different images as shown in Fig. 2-6 b). However, double-screen function is designed with a planar mirror attached for observers to perceive two different images at the same time as shown in Fig. 2-8. Since dual-view and double-screen functions are the medium in generating two images, the methods used in dual-view function can be implanted in double-screen function.

The proposed 3D double-screen display, as shown in Fig. 2-8, consists the top screen, a panel with micro-optical structure attached as shown in Fig. 2-9, and the bottom screen, a mirror. Each screen is designed to create the independent 3D images. Thus, the micro-optical structure needs to have both 3D and double-screen functions, which means to have the ability to re-direct the incident light to the specific viewing regions. Therefore, the design concepts and working principles need to be further investigated.

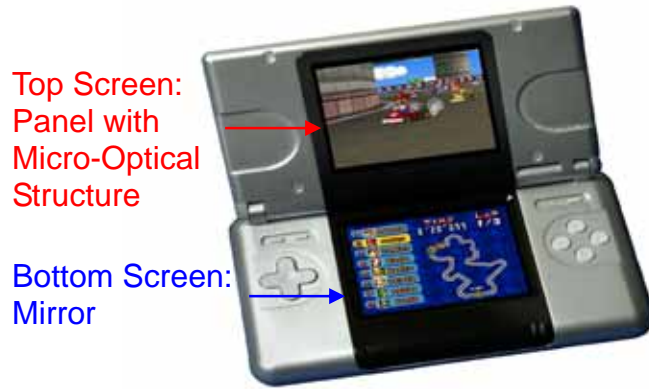


Fig. 2-8. Concept of the proposed 3D double screens display system.

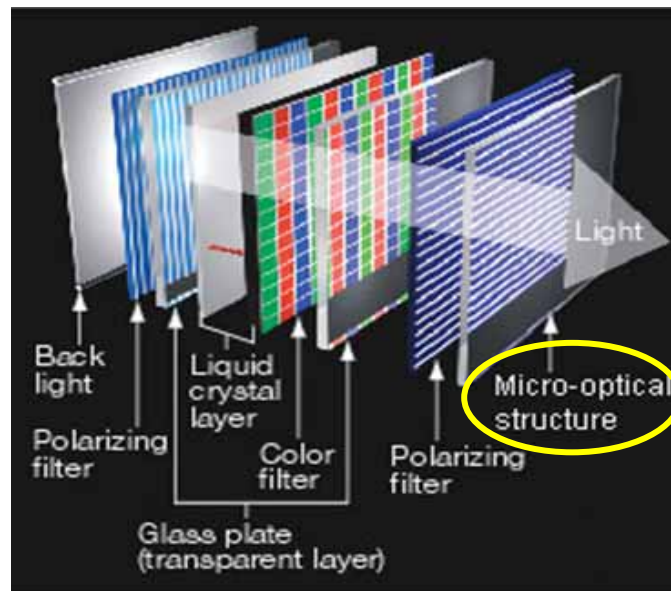


Fig. 2-9. Configuration of the top screen with micro-optical structure.

2.5.1 Model Adopted

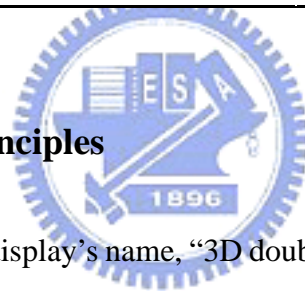
After the evaluation of various 3D methods, the spatial-multiplexed method including parallax barrier and lenticular-screen has been chosen to be the candidate in our research. By comparing the products using lenticular-lens and parallax-barrier, lenticular-lens seems to be more attractive to our preference. The brief results of products using lenticular-lens and parallax-barrier are shown in Table 2-2 [33].

Notwithstanding parallax barrier can block the undesired image sectors, the brightness and resolution of entire viewing images will be reduced. Besides, although lenticular-lens has similar result on reducing the resolution, the generated split images have smaller crosstalk and higher brightness. Thus, lenticular-lens is a better option to enlarge the viewing angle in our design.

Table 2-2. Comparison of displays using lenticular-lens and parallax-barrier.

Parameters	Parallax Barrier	Lenticular Lens
Crosstalk	2% ~ 10%	< 1% 👍
Brightness	< 50%	> 100% 👍
Resolution	50%	50%

2.5.2 Functioning Principles



As implied by the novel display's name, "3D double-screen display" needs to have 3D and double-screen functions. In order to accomplish both functions, we can combine a layer performing 3D function and another layer with double-screen function. In addition, the proposed system has top and bottom screens. According to Snell's Law of refraction, the information which contains top and bottom screens images can be split by the functional layer to the respective screen in the top or bottom direction, respectively. In order to see images on both screens at the same time, the bottom screen is designed to be a mirror. According to the Law of Reflection, the mirror could be used to redirect the images to the observer. The observer can view top screen images directly from the panel and bottom screen images from the mirror simultaneously.

Besides, 3D image contains left and right eye's images. The 3D functional layer has to direct the respective images to each eye in left and right directions. Hence, in combining both functions together, both layers of lenticular-lenses have to be located perpendicular to each other as shown in Fig. 2-10. 3D and double-screen functions will then be appeared simultaneously in horizontal and vertical directions, respectively. Consequently, the lenticular-lens-based micro-optical structure including two functional layers of lenticular-lenses dominates the light source of the display system will be the most important part of this study.

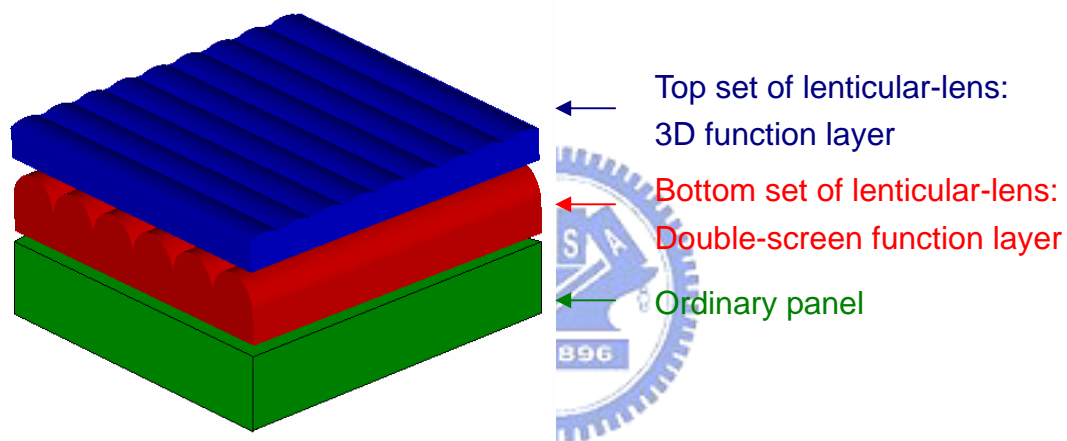


Fig. 2-10. Schematic of the micro-optical structure.

2.6 Applied Fields of 3D Double-screen Display

There are many fields can be applied the proposed 3D double-screen display on. The most effective examples for getting the benefits from the design are listed in Table 2-3.

Table 2-3. Possible fields of using 3D double-screen display.

Applied Fields	Description
Personal TV and monitor	
Industrial instrument	
Medical imaging	
Arcade game	Having a screen shows the picture images while another screen describes the reference data.
CAD/CAM	
e-Business	
Education and exhibition	
3D map of vehicle control	
Stereo video phone and mobile phone	

2.7 Summary

After reviewing the 3D vision principles and display technologies, a new system model is proposed by utilizing lenticular-lens as medium of the micro-optical structure to perform dual-functioning on a single unit. By pasting the micro-optical structure onto a panel and adding on a mirror, the system can generate two diverse images without shrinking their scales in a single display. Users can watch the TV program on a panel and use another one to track the information on internet. This innovative feature is applicable to the products such as notebook PCs, mobile phones and hand-held devices etc. with convenience and cost advantage of showing two information channels simultaneously. The accuracy of presented images, which is heavily depended on the shape and size of lenticular-lens, is the objective of the research. Due to lens' profile affected by the pixel size, the layout styles of color filter are examined. In order to yield better viewing performance, the optimized design and

simulations of the micro-optical structure will be further studied and analyzed in Chapter 3.



Chapter 3

Design of Lenticular-lens-based Micro-optical Structure for 3D and Double-screen Functions

3.1 Introduction

The lenticular-lens based micro-optical structure can be used to re-directing the incident light from the panel and functioning 3D and double-screen images. However, the uncertainty of the lens design may narrow down the viewing angle and result the images in the unexpected viewing zones [24, 25]. The unexpected position of an image causes the interference with the other image, as called crosstalk [26]. Thus, the design on lens-based micro-optical structure is very important for generating the 3D and double-screen images.

3.2 Optical Design of Micro-optical Structure

The micro-optical structure contains two lenticular-lens layers for functioning 3D and double-screen images. In order to operate precisely and obtain the images correctly, pixel size, viewing distance and viewing angle have to be considered in designing the micro-optical structure. Thus, the novel system structure has proposed and the related equations have derived. Finally, the further adjustment on these parameters can result an optimized viewing performance.

3.2.1 Lens Design

One of the advantages using lenticular-lens is having the magnification ability. Because the spatial-multiplexed method requires a single image to be split into left and right sides images, there will occur the black strips in that empty slots. However, the magnification ability of the lens will cover them to provide a continuing image in the spatial domain. The magnification m of the lenses is given by the ratio of the interocular distance e and the LCD pixel pitch i . Geometrically, this ratio is also the ratio between z and f .

$$m = \frac{e}{i} = \frac{D}{f} \quad (3-1)$$

As with parallax barrier displays, the effective of viewpoint to see the correct left and right images is determined by pixels at the edge of the display. The lenticular-lens based 3D displays, however, have a little difference on determining the effective viewing zone as illustrated in Fig. 3-1 [34]. The lenticular pitch needs to be set so that the centre of each pair of pixels is projected to the centre of the viewing windows [34]. The specific parameters of the lenticular-lenses are the lens pitch l and the viewing distance z . The relationship between pixel pitch i and lenticular-lens pitch l can be found by considering similar triangles.

$$\frac{2i}{z} = \frac{l}{z - f} \quad (3-2)$$

After sorting the equation,

$$l = 2i \left(\frac{z - f}{z} \right) \quad (3-3)$$

Typically the pixel pitch is set by the choice of ordinary display and the minimum focal length, f , determined in large part by the substrate thickness on the front of the display.

The distance, z , between the color filter and the observer has the relationship by considering the other similar triangles,

$$\frac{i}{f} = \frac{e}{z - f} \quad (3-4)$$

By reorganizing the equations,

$$z = f \left(\frac{e}{i} + 1 \right) \quad (3-5)$$

Typically the average human eyes' separation distance, e , for normal people is around 65 mm. Since eye separation distance and pixel pitch are constant, the viewing distance is relied on the focal length of our design. From equations 3-3 and 3-5, the lens pitch can be estimated with the best viewing distance declared. In addition, the triangle consisting human eyes' separation distance and viewing distance also provides the relationship with viewing angle.

$$\theta = \tan^{-1} \left(\frac{e}{D} \right) \quad (3-6)$$

By imaging a little triangle in the lens, the lens radius, C , can be found in terms of lens pitch and its thickness.

$$C = \frac{\left(\frac{l}{2}\right)^2 + 4(z - f - D)^2}{8(z - f - D)} \quad (3-7)$$

The region where $(z - f - D)$ is the lens thickness and can be defined as the distance between the curviform and flat surfaces. The half width of the lens can be represented as $(l / 2)$. Therefore, the lens radius can be extracted by measuring the half width and lens thickness.

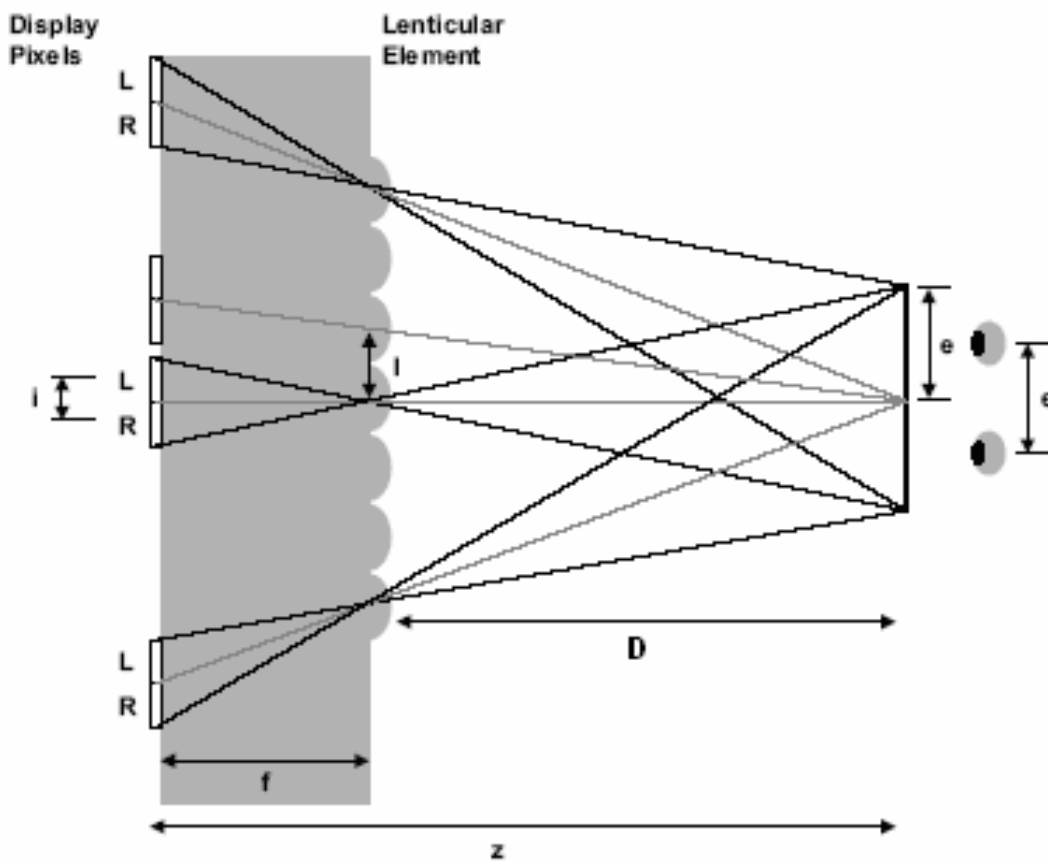


Fig. 3-1. Schematic of lenticular-lens based 3D display.

3.2.2 Functions Design

In order to have 3D images, the viewing screen for each eye has to be small enough to cover only one eye in the region. As the result, if two eyes are seeing the same view, the 3D image will be simplifying as a 2D image. Therefore, the principle of functioning double-screen images is to enlarge the 3D viewing screen horizontally to contain two eyes in the entire path of each observing directions. Hence, the left and right eyes' 3D images will soon become the left and right directional multi-viewing images. The double-screen function is, thus, created.

Lens pitch is one of the significant subdivisions of lens design. When the size of structure's lens pitch matched the display's pixel pitch, 3D images are generated as shown in Fig. 3-2 (a). In the other approaches, the larger lens pitch has increased the size and decreased the number of light spots. Therefore, when the lens pitch for double-screen function is practically twice of the 3D pixel size, the results are shown in Fig. 3-2.

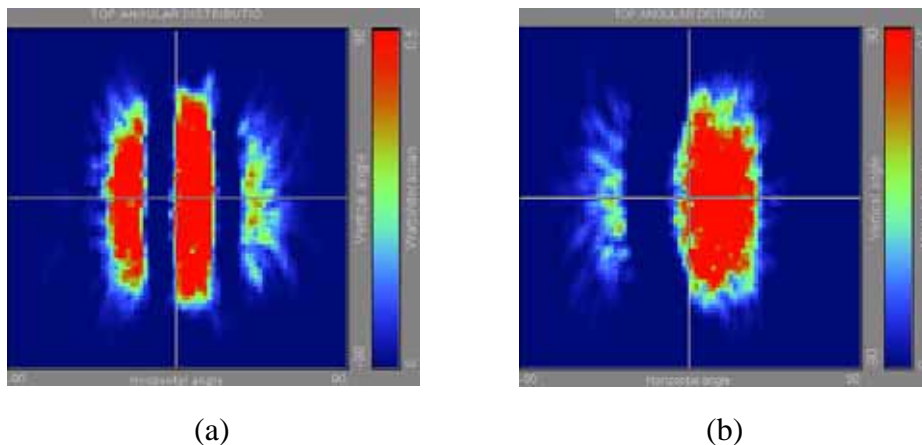


Fig. 3-2. Lens pitch of (a) 594 μm for 3D and (b) 1188 μm for double-screen image.

3.2.3 Structure Design

The wider viewing angle means to have the larger lenticular-lens pitch.

Correspondingly, the pixel pitch of the ordinary TFT-LCD which has the color filter structure layout in portrait [30], as shown in Fig. 3-3, has to be increased. Therefore, when the layout of color filter was swapped from portrait to landscape as shown in Fig. 3-3, the increased of relative lens pitch could yield double-screen function.

Consequently, the key point of getting 3D images or dual-view images is the configuration between color filter and the lenticular-lenses as parallel or vertical. Because there is only one color filter layer, the direction of lenticular-lens for both functions will be perpendicular to each other. Since the aligning direction is different, there is no conflict in combing both function layers together. Thus, the micro-optical structure consists both functions will generate 3D and double-screen images in the proposed display system.

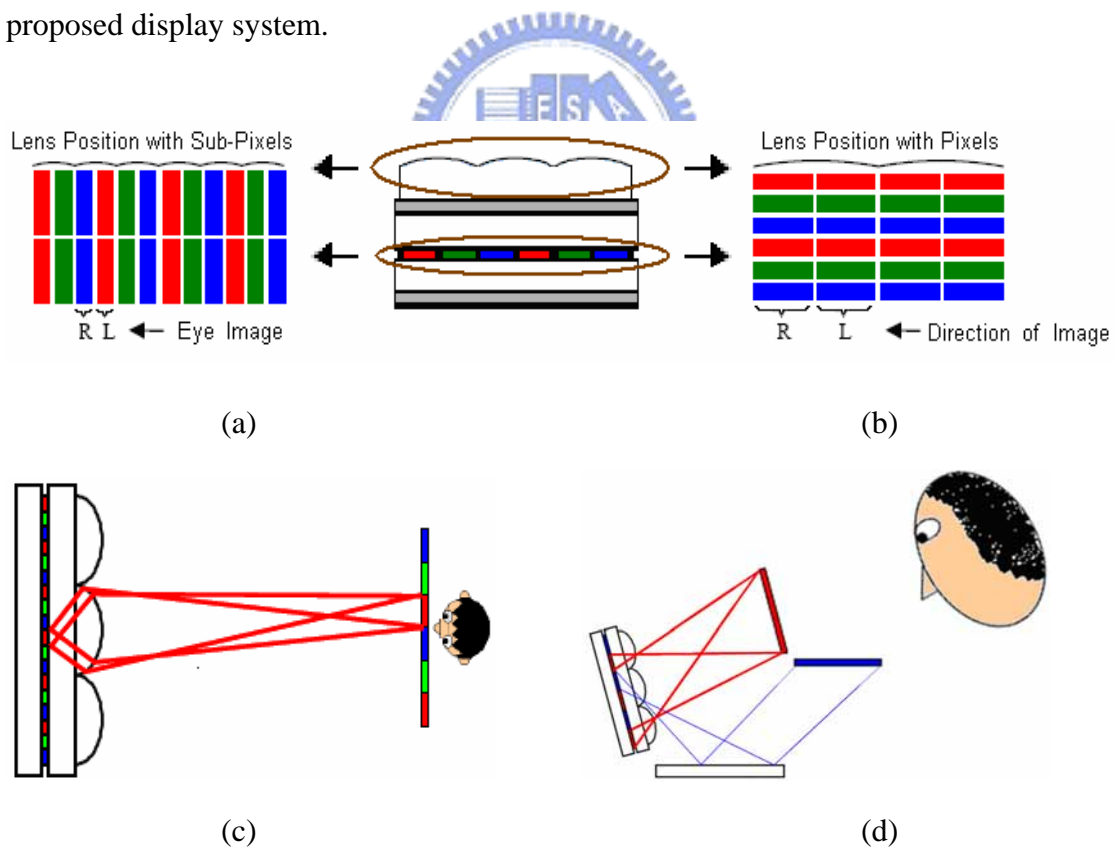


Fig. 3-3. The structure layout of lenticular-lenses with color filter's pixels (a) in portrait and (b) in landscape with respected theoretical images of (c) portrait for 3D and (d) landscape for double screens.

3.3 Image Quality

The image quality of either 3D or double-screen function depends on the width of acceptable viewing range. If information received the disturbance from the opponent side, the interference portion may not be viewable and shall be excluded for counting as acceptable viewing angle range. Hence, the decreased viewing zone may cause the problem on maintaining the proper function of each designed layer. The study on image quality, thus, has to consider the acceptable viewing angle range and crosstalk issue.

3.3.1 Crosstalk Issue

In order to have better image qualities, the lenticular-lenses have to precisely direct the specific directional images to that direction only. For example, the right eye's images have to go to the right eye, and should not be received by the left eye. However, there are always the possibility of two images interfered with each other, as name crosstalk.



Crosstalk, defined as the ratio of brightness measured at one directional image to the other [29], is an important variable to distinguish the level of clearness and precision of viewing images. If one direction's image crossed over to another direction's viewing screen, and the overlap regions will appear the blurred image. Hence, in order to have clear and large viewing screens, the crosstalk ratio of less than 10 % is the minimum criterion to produce stereoscopic image perception for our brain [29].

$$\text{Crosstalk} \equiv \frac{\text{Luminance measured at one direction image}}{\text{Luminance measured at the other direction image}} \quad (3-1)$$

There are two types of images interference. The delimitation can be given to the luminance occurred near opposite side of 0° vertical line as light-leakage, and the jumped out crosstalk as light-spot as shown in Fig. 3-4.

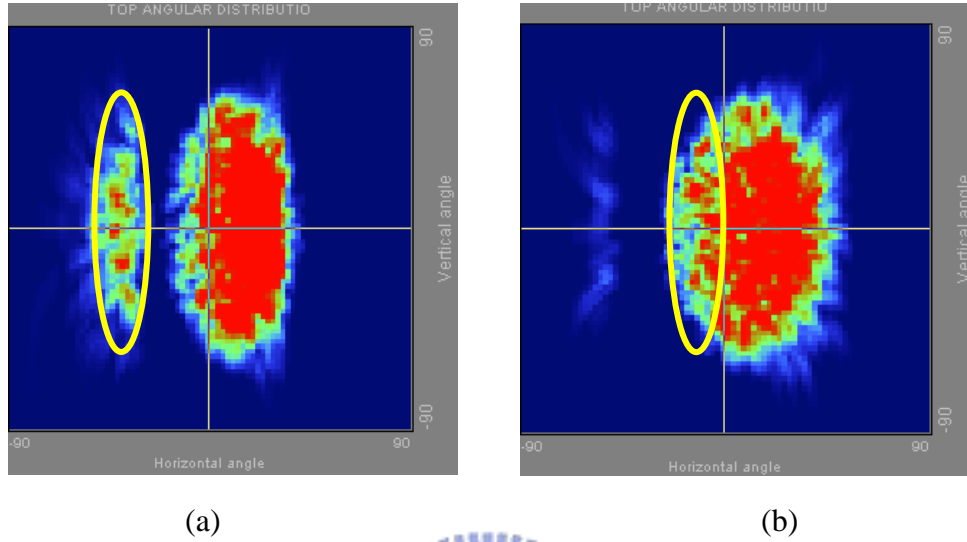


Fig. 3-4. Definition of crosstalk as shown in circle: a) light-spot and b) light-leakage.

3.3.2 Determination of Acceptable Viewing Angle Range

In the display system, viewing angle is used to be a major parameter to determine the display performance. By considering the crosstalk issue, the overlapped parts from image splitting result for each direction has to be excluded as the acceptable viewing angles as shown in Fig. 3-5. The figure shows the acceptable viewing angles for right directional image are only from approximately 10° to 40°. These 30° portion will have the crosstalk ratio of less than 10% and provide a clear image. Thus, the true viewing angle range for the observer should be 30°, not 60° as counted from -10° to 50°. In this study, the range of acceptable viewing angles is the most important parameter in the evaluation and is written in short as “viewing angle.”

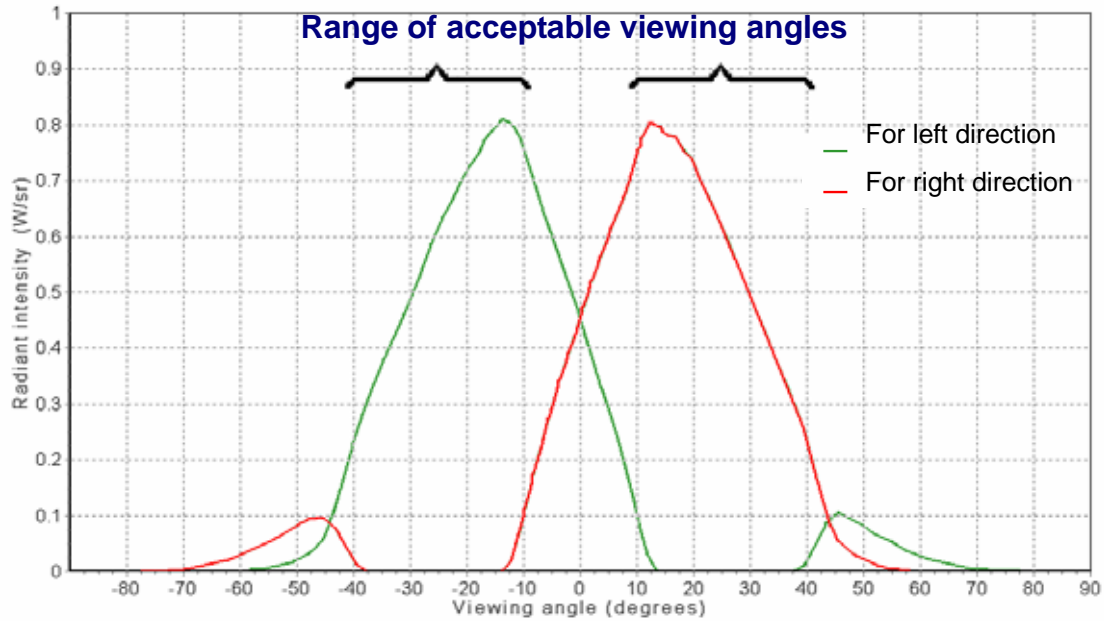


Fig. 3-5. The range of acceptable viewing angles after considering the crosstalk.

3.4 Optimizing Viewing Performance

In order to obtain an optimized 3D double-screen performance, some parameters of the micro-optical structure have to be adjusted, such as the micro-optical structure's thickness and the lenticular-lens radius. Since these parameters affect the 3D and double-screen appearances, each effect are discussed in later sections and are summarized in Table 3-1.

Table 3-1. Comparison of 3D and double-screen functions' parameters.

Parameters	3D Function	Double-screen Function
Substrate Thickness	Thicker	Thinner
Material Refraction Index	Smaller	Larger
Lens Pitch	Smaller	Larger
Lens Radius	Larger	Smaller

3.4.1 Material Refraction Index Effect

Most of the colorless materials have material refraction index around 1.5. According to this value, the parameters for 3 views 3D function, as shown in Fig. 3.6 (d), are founded and set as constant value for advanced experiment on utilizing different material refraction index. When the index is getting larger, the angular distribution of light intensity is gathering closer to the certain viewing angle regions as shown in Fig. 3.6 (a). The double-screen function could be created. Nevertheless, the reduced index value caused several light spots. The light spots are first appeared at the opponent side, and then yielded more and more light strips. As the result, the multi screens 3D images is established as shown in Fig. 3.6 (e).

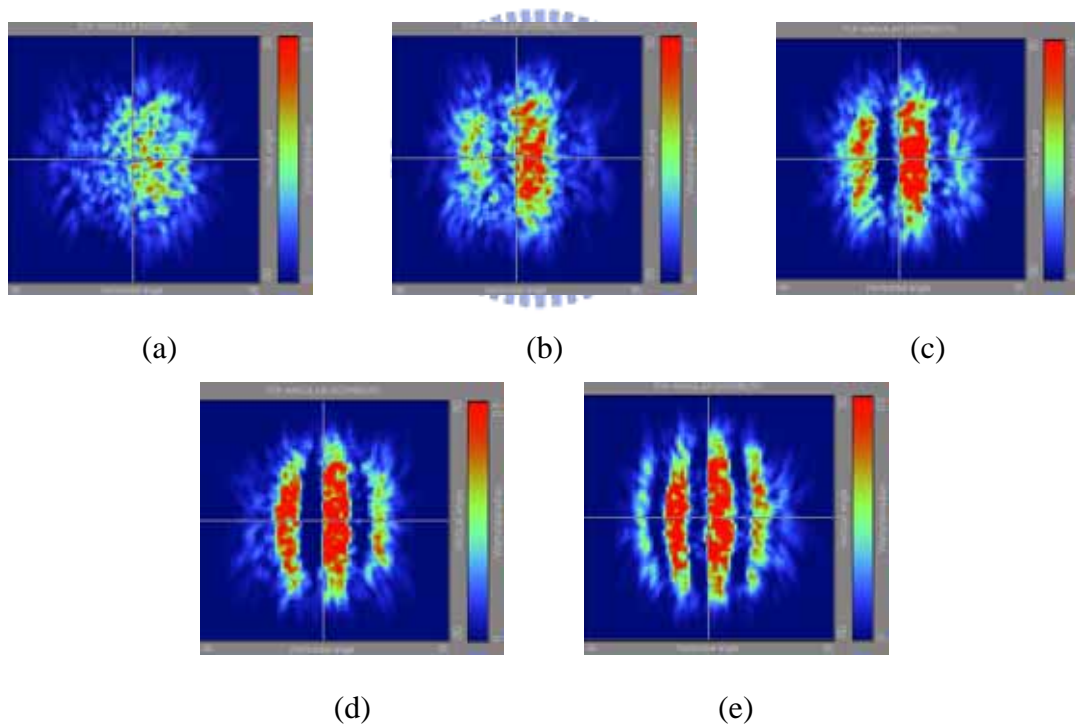
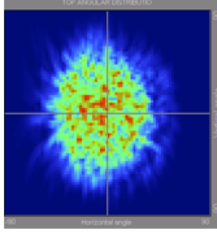
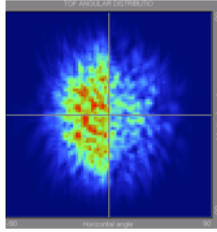
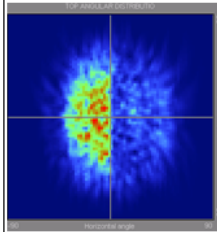
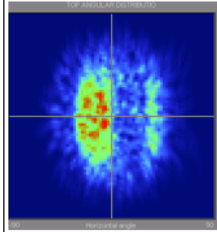
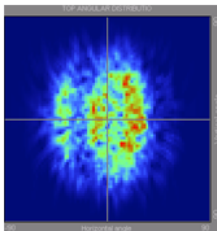
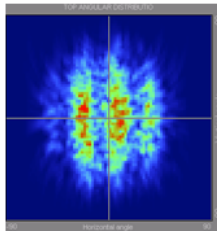
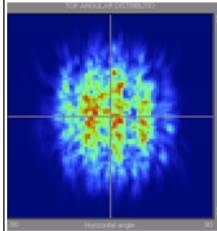
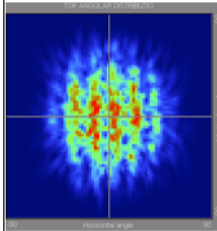


Fig. 3-6. Results of right eye's 3D or right direction double-screen images with varies material refraction index: (a) $n=3$, (b) $n=2$, (c) $n=1.7$, (d) $n=1.5$ and (e) $n=1.3$.

3.4.2 Substrate Thickness Effect

The substrate thickness including glass and micro-optical structure plays a major role in having 3D or double-screen function for the lenticular screen. Table 3-2 shows the lens based functional layer has favoring in producing 3D than double-screen images when the substrate is thicker. Moreover, if the layers of glass and micro-optical structure are too bulky, the thickness becomes an issue in generating light-spot in the double-screen image as shown from the result of thickness equal to 180um. As the layers are thinner, the light-leakage takes larger portion of viewing angles for the 3D image as shown from the result of 900um thickness. Thus, the 3D and double-screen functions are favor in thicker and thinner substrates, respectively.

Table 3-2. Substrate thickness with its respected light intensity distributions.

Thickness	10 um	80 um	130 um	180um
Results				
Features	2D image	D-s image	D-s image	D-s image
Thickness	300 um	500 um	700 um	900um
Results				
Features	Trans. image	3D image	3D image	3D image

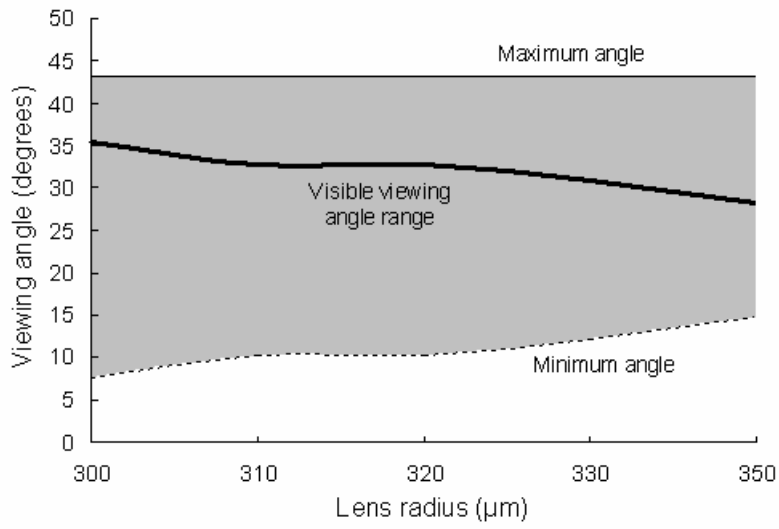
Furthermore, the substrate thickness is sometimes undesirable. The best candidate may be the substrate closing to the anticipated thickness. Therefore, crosstalk issue is

insufficient to be avoided completely and has to adjust the lenticular-lenses or other parameters for an optimized performance.

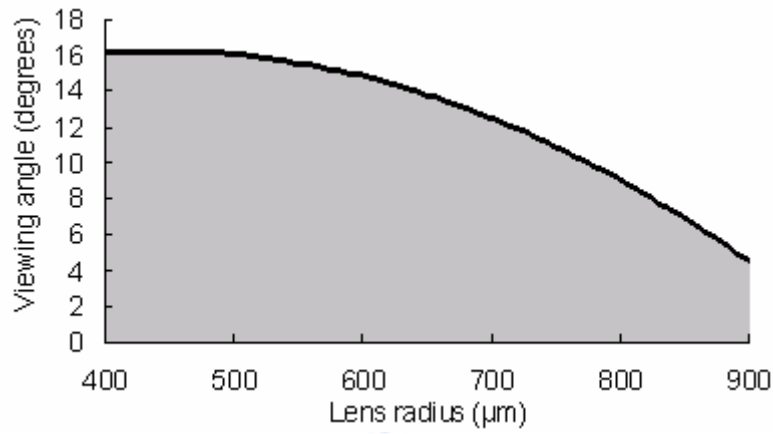
3.4.3 Lens Radius Effect

After decided the thickness and clarified the lens pitch, the major issues are on modifying the lenticular-lens curvature to avoid light-leakage and light-spot. From the simulated results as shown in Fig. 3-7 (a), a larger lens radius has smaller visible viewing angle range. Since the maximum viewing angle is fixed, the acceptable viewing angle range would depend on the minimum visible angle. In the other words, viewing the image from smaller degrees of viewing angle is available after reducing the amount of crosstalk region, which implied that the possible solution is to decrease the lens radius. Therefore, by reducing the lens radius, the crosstalk portion can be reduced, and wider viewing angle can be obtained.

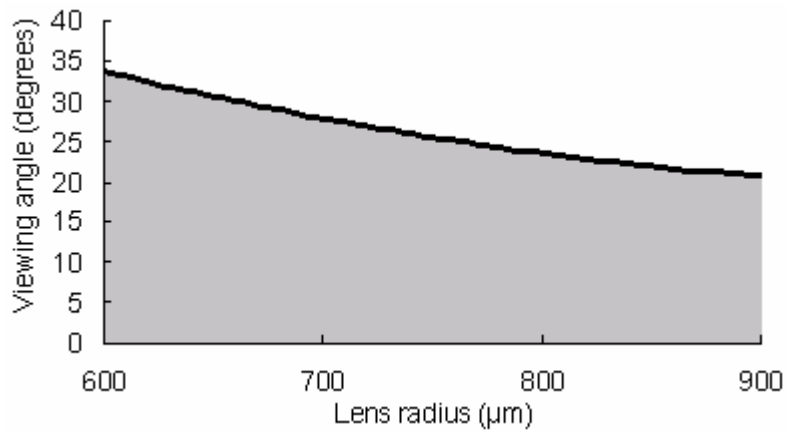
After examining the definition of the visible viewing angles range in the general case, the figures of relationship between lens radius and viewing angles for 3D and double-screen functions can be established. In the 3D function, the relationship curve starts to decay after 500 μm as shown in Fig. 3-7 (b). The double-screen function has the decreasing slope approaching to the linear line as shown in Fig. 3-7 (c). In short, the resulted visible viewing angles are inversely proportional to the lens radius for both 3D and double-screen functions. In order to have larger acceptable viewing angle, the lens radius needs to be smaller.



(a)



(b)



(c)

Fig. 3-7. Relationship between the lenticular-lens radius and viewing angles for (a) general case, (b) 3D function and (c) double-screen function.

3.5 Simulations

In order to have 3D double-screen display, the functional layers of generating 3D and double-screen images need to be evaluated. Therefore, 3D and double-screen functions were modeled and analyzed by the optical designs program “ASAP 7.5.” The angular distributions of 3D and double-screen functions were simulated on a 1” panel with the resolution of 72 x 48 and the active area of 21.4 X 14.3 mm². The simulation parameters of lenticular-lenses arrays are listed in Table 3-3.

Table 3-3. Calculated 3D double-screen display parameters.

Items	Symbols	Parameters for 3D	Parameters for D-s
Object Size	x	6.5 cm	13 cm
Combined pixel pitch	i	99 μ m	198 μ m
Magnification	m	657	657
Lenticular-lens pitch	l	594 μ m	1188 μ m
Viewing distance	D	25 ~ 40 cm	25 ~ 40 cm

3.6 Simulated Results and Discussions

The simulated results include three parts, 3D function, double-screen function and their combination. Each section should operate properly in order to achieve the final target of generating 3D double-screen images.

3.6.1 3D Function

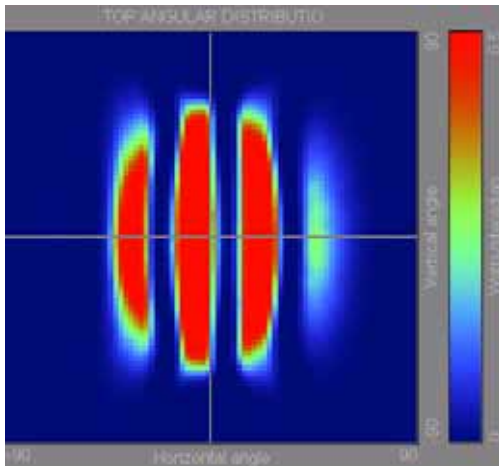
The viewing angles for distance at 25 cm and 40 cm are estimated by equation 3-6 and are $\pm 14^\circ$ and $\pm 9^\circ$, respectively. The schematic diagram is illustrated in Fig.

3-8. In addition, the simulation for left and right eye's images of 3D function are done for observing position at 25 cm, and its results are shown in Fig. 3-9. There are 3 light strips generated. Each strip has the width about 14° after deducted the overlapping more than 10% crosstalk portions with the opponent direction. The viewing angles of simulated results have perfectly matched the design. Moreover, a region consists a pair of left and right eye's 3D images is called viewing zone. The simulated result as shown in Fig. 3-9 indicates 3 pairs of light spots for left and right eyes. Thus, an observer can view the 3D images from 3 different horizontal directions.

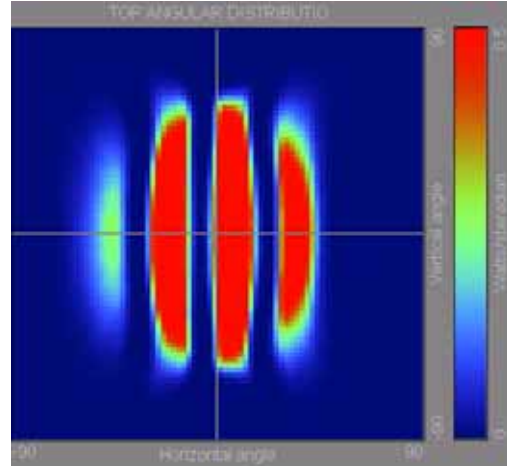
Since the simulation program is set with the maximum light transmitted to be 1 W/sr as 100% transmittance. When the observer stands at the center viewing zone, the light intensity perceived by eyes will be the maximum amount as shown in Figs. 3-9 (c) and (d). Other than the light strip with highest intensity among all, the other two peaks aside as for the other viewing zones are still viewable since their light efficiency is more than 50% of the total input. Moreover, the light intensities for left and right images are similar. Because the maximum differences are less than 10% of each other, human will not sense the variance of the images. Consequently, observers could view the 3D images in 3 viewing zones, which are the center and 30 degrees at each side of the display.



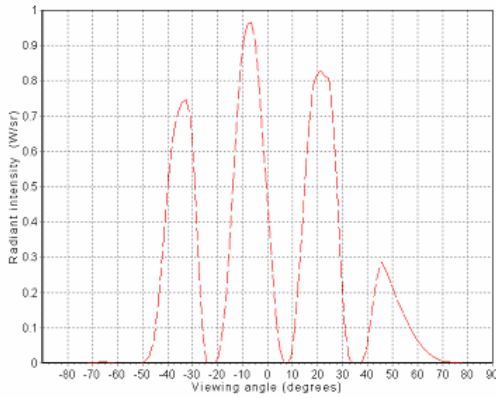
Fig. 3-8. Schematic diagram of viewing angles at near and further viewing positions.



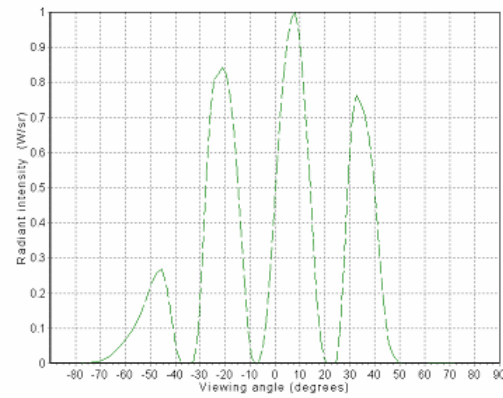
(a)



(b)



(c)



(d)

Fig. 3-9. Angular distribution of proposed 3D function for (a) left and (b) right eye's image, and (c) and (d) are their respected cross-section intensity distribution in horizontal orientation.

3.6.2 Double-screen Function

By using ASAP to simulate the design model, the optimized angular distribution of double-screen function has been found for bottom and top screens as shown in Fig. 3-10. The valid viewing angle is derived ranging from approximately 0° to 40° for each direction. However, the maximum acceptable viewing angle range was found to be 30° after considering the crosstalk issue. Because the range of viewing angle is larger for double-screen function, the light efficient is less than 3D function. Notwithstanding,

there are still a large amounts of light transmitted with more than 50% of efficiency as shown in red center region of Figs. 3-9 (a) and (b). The top and bottom screens have the similar light efficiency as shown in Figs. 3-9 (c) and (d). All in all, since both screens can be functioned at similar viewing angle, the observer could view two images at the same time with 30° viewing freedom vertically.

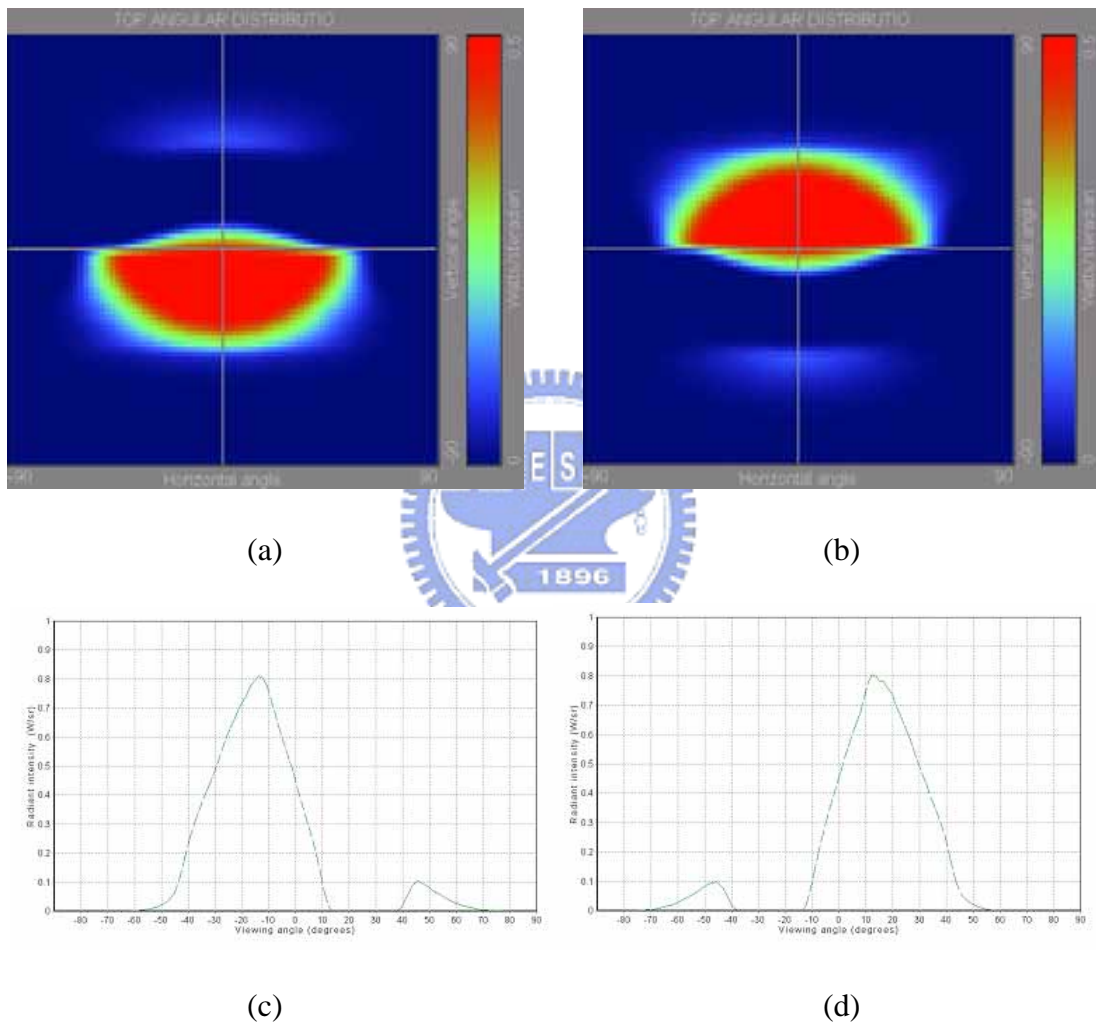


Fig. 3-10. Angular distribution of proposed double-screen function for (a) bottom and (b) top direction image, and (c) and (d) are their respected cross-section intensity distribution in vertical orientation.

3.6.3 3D Double-screen Function

The simulated results of 3D double-screen display represent the combination of 3D and double-screen features. Due to human's eyes perception, the crosstalk needs to be of less than 10 %, hence, viewing-angle ranges are around $-35^{\circ} \sim 35^{\circ}$ and $\pm 5^{\circ} \sim \pm 40^{\circ}$ in the horizontal direction and vertical direction, respectively, as shown in Fig. 3-11. The angular distribution of light intensity for each screen is shown in Fig. 3-12.

Because the 3D function layer is designed to place on the top of double-screen function layer, the thickness is thicker than operating 3D images alone. Since the 3D function is favorable for bulky substrate, the larger distance between the 3D function lenses arrays and color filter enhanced more views of 3D images. Thus, in the proposed 3D double-screen design, there are roughly 6 views generated. Due to the low light intensity at very left and very right viewing zones, the images at these two zones may not be perceivable. The overall amounts may end up with 4 clear viewing zones horizontally for both top and bottom screens.



Fig. 3-11. Schematic diagram of acceptable viewing-angles for top and bottom screens.

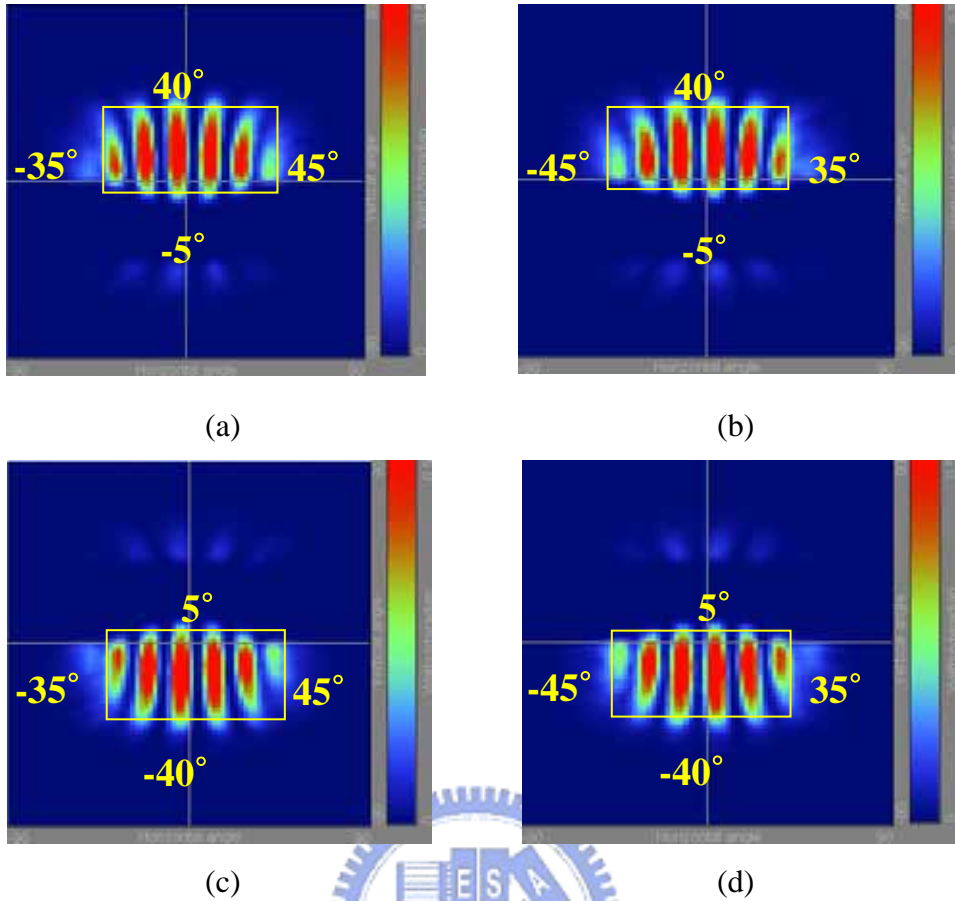


Fig. 3-12. Angular distributions of the proposed 3D double-screen display for (a) left and (b) right eye's images of top screen; (c) left and (d) right eye's images of bottom screen.

3.7 Summary

The intention of research is to design a lenticular-lenses-based micro-optical structure generating dual 3D images simultaneously. The principles of producing 3D and double-screen images have been investigated. Hence, 3D and double-screen functions have designed to align with color filter in portrait and landscape orientation and to direct the incident light to the desired regions. In addition, the investigation on proposed structure shows 3D function is favoring thicker substrate, smaller material refraction index, smaller pitch and larger lens radius, which is opposite to double-screen function's favors. After considering the parameters of potential threats

to the range of viewing angles, the performances of 3D and double-screen functions have been optimized. Moreover, the simulated results of 3D and double-screen functions and their combination have verified the proposed concept. The micro-optical structure consists 3D function layer and double-screen layer are generated at least 4 viewing zones of the clear 3D images with viewing angle range around $-35^{\circ} \sim 35^{\circ}$ and $\pm 5^{\circ} \sim \pm 40^{\circ}$ in the horizontal direction and vertical direction, respectively. Thus, by including the planar mirror in the optical system, observers can view 3D images at top and bottom screens simultaneously.



Chapter 4

Fabrication of the Lenticular-lens-based Micro-optical Structure by Excimer Laser Micromachining System

4.1 Introduction

The fabrication technologies of micro-optics are getting more and more advanced. Fabricating the more flexible components and system designs, such as smaller and precise structures, becomes possible. A large variety of materials is available, ranging from glass to semiconductor materials and on to plastic. The technologies to fabricate micro-optical elements can be simply classified into two main categories, lithographic and non-lithographic techniques. Lithography is the name for a sequence of processing steps, pattern generation, coating or thin layer deposition, alignment, and exposure, pattern transfer for structuring the surface of planar substrates.

In the 1970s planar lithographic fabrication techniques were adapted from semiconductor process to the fabrication of optical elements, for example, to fabricate special beam splitters and lens arrays. The use of these techniques allows one to generate optical component with dimension in the micrometer range. Besides, in an effort to fabricate some specified elements such as micro-lens, non-lithographic techniques, for example, diamond cutting and micro-jet printing have been investigated. However, these techniques often do not have small enough critical dimensions or are unable to generate the micro-optical element with inadequate designed surface relief. Other than that, the fabrication time and cost are also the issues.

In terms of recent fabrication technology, the economical processes with satisfying the requirements on fabricating the lenticular-lenses arrays have to be discovered and developed. Since excimer laser ablation is a rapid and effective way for micromachining a surface relief onto a substrate material, the study will be progressed based on utilizing the excimer laser system to fabricate the lenticular-lens-based micro-optical structure.

4.2 Fabrication Principle

In order to make possible of fabricating lenticular-lenses by the excimer laser micromachining system, the process steps, system structure and micromachining principle are explored.

4.2.1 Fabrication Process



There are several fabrication techniques. The most common fabrication processes of lithography technology needs 6 steps as shown in Fig. 4-1. First the photosensitive materials like photoresist are coated on the substrate. The modulated illumination for desired pattern is applied to expose the photoresist. After exposure, a development step converts the exposed photoresist onto a surface profile. In a further processing step, the surface profile of the photoresist pattern can be transferred into the substrate. Consequently, the micro-optical elements can be fabricated with above procedures on the substrate.

The intention of this research is to fabricate the lenses by excimer laser micromachining system which has advantage in shorter duration time and simpler process steps of fabrication as shown in Fig. 4-2. The initial and final clean of the

substrates are the only steps similar to the general lithography method. The step of excimer laser micromachining combined several lithography processes includes exposure and etching in a single step. PR coating and development are not necessary to be part of process any more. In addition, the fabricated substrate will be cleaned by Ultrasonic Cleaner with Isopropyl Alcohol. The inspection of the patterns can be evaluated through microscope and Zygo's interferometer.

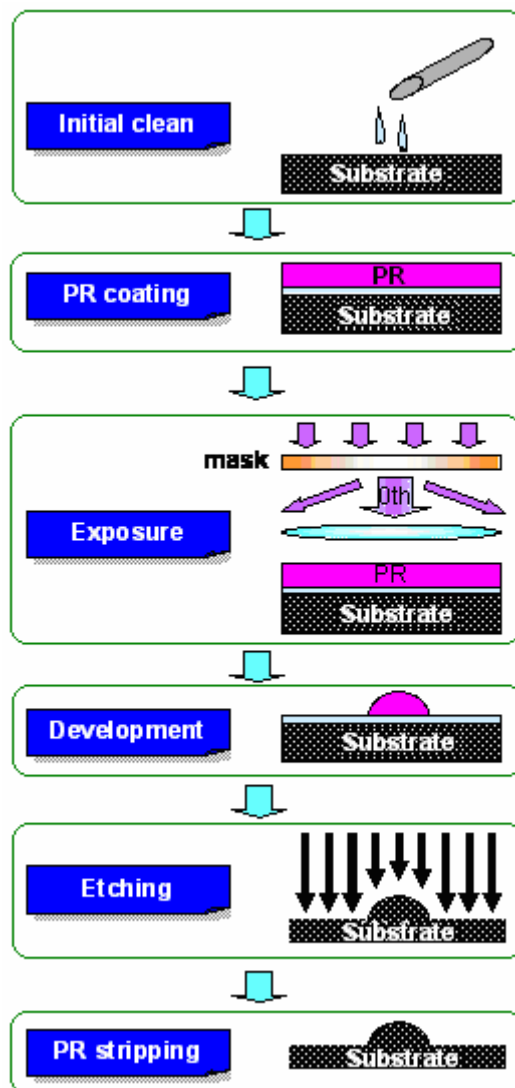


Fig. 4-1. Detailed fabrication processes of general lithography technology.

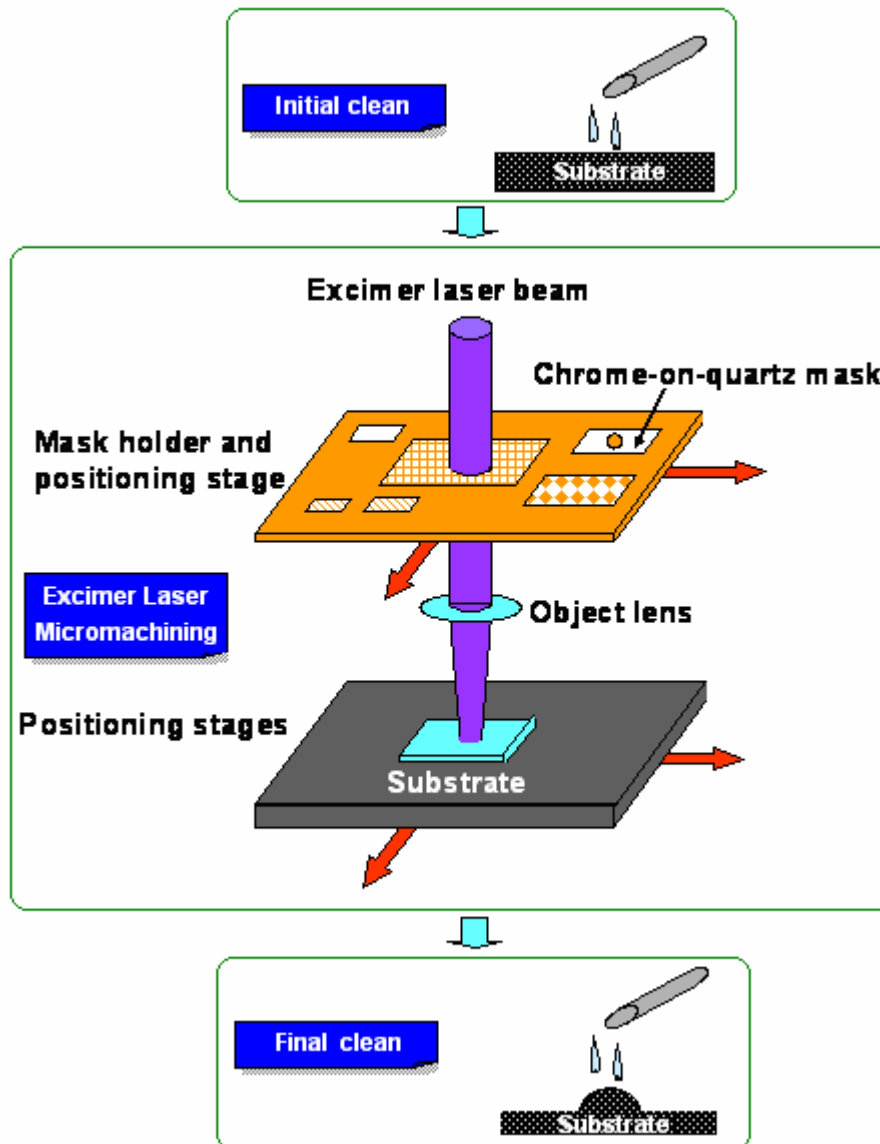


Fig. 4-2. Detailed fabrication processes of excimer laser micromachining technology.

4.2.2 Excimer Laser Micromachining System

The excimer laser micromachining system consists several components as shown in Fig.4-3. The utilized laser is a Kr F excimer laser operating at 248nm. The maximum energy per pulse is typically equal to 0.7 J, the pulse duration is approximately 20ns, and the maximum repetition rate is 100Hz. In order to let the machining energy be programmable, the emitted excimer laser beam first passes through the attenuator, and the value of attenuator is between 0 and 1 controlled by

the program. Because the intensity profile of an excimer laser output is quite non-uniform, beam forming optics and beam homogenizer inside beam delivery system are used to produce a uniform intensity field at the mask plane. This step can create a highly uniform ($\pm 5\%$ RMS) illumination of $12 \times 12\text{mm}$ at the mask plane. Then the mask plane is imaged on the substrate to ablate the polymer substrate with 4x or 10x demagnification by UV objective of a 0.1 or 0.2 NA respectively.

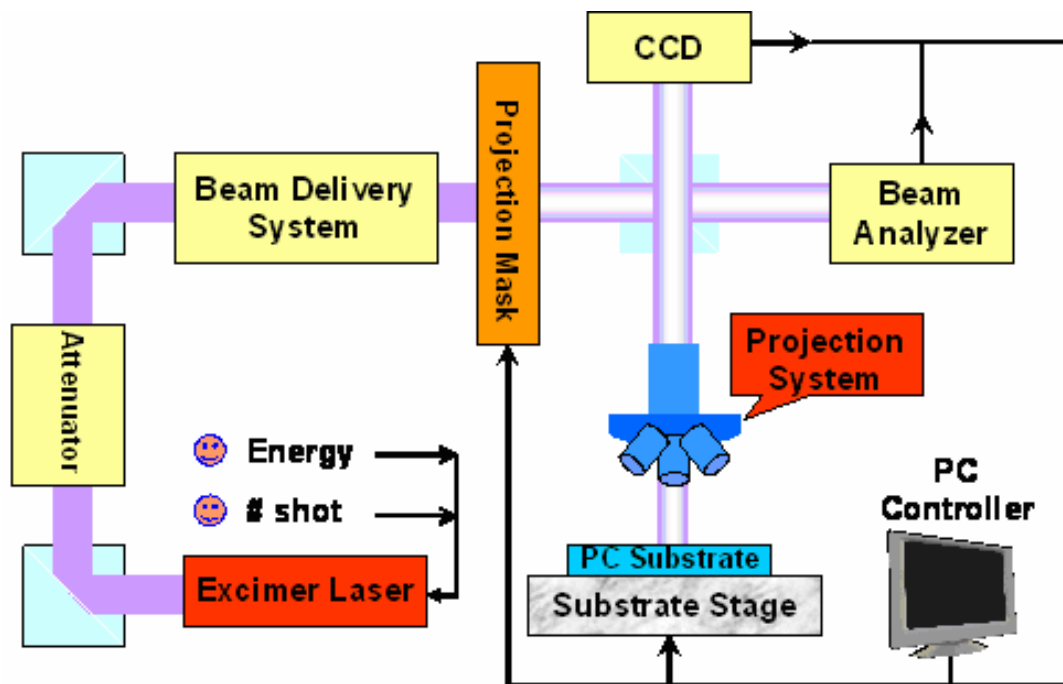


Fig. 4-3. Schematic diagram of excimer laser micromachining system.

4.2.3 Micromachining Technique

The structures are created by scanning the image of the contour mask across the substrate while operating the laser with a fixed pulse repetition rate. The principle of this method is that only the mask contour defines the locally applied laser pulse quantity. The region with more excimer laser passed through the contour mask will result deeper depth. The detail process is shown in Fig. 4-4. More complex structures can be achieved by subsequent scan step. In this way, lenticular-lenses and

lenticular-lenses arrays are expected to be fabricated by scanning in orthogonal directions with a containing semi-circular shape contour mask as shown in Fig. 4-5.

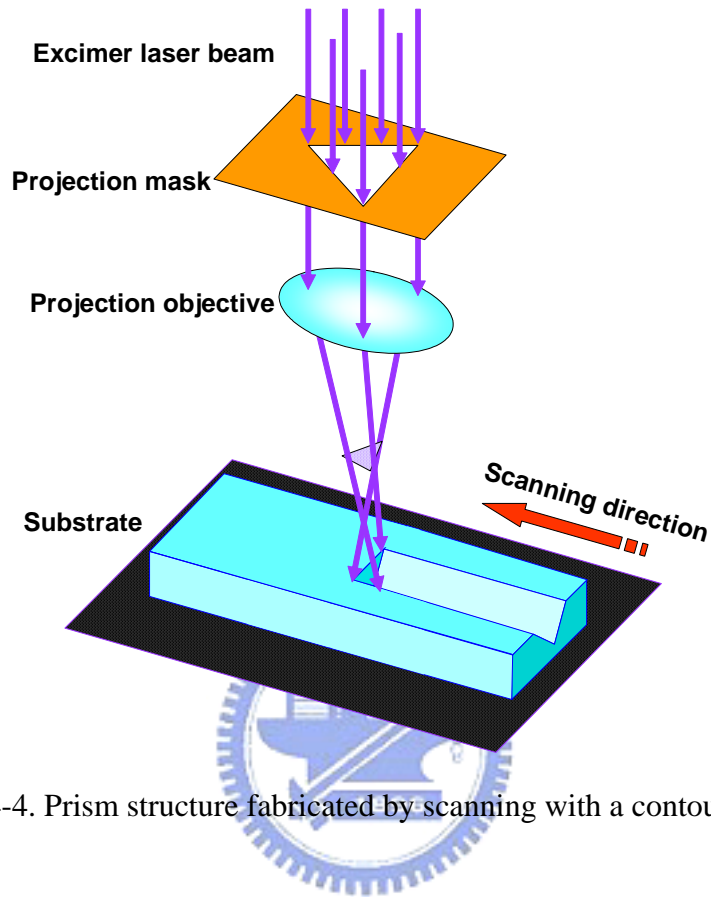


Fig. 4-4. Prism structure fabricated by scanning with a contour mask.

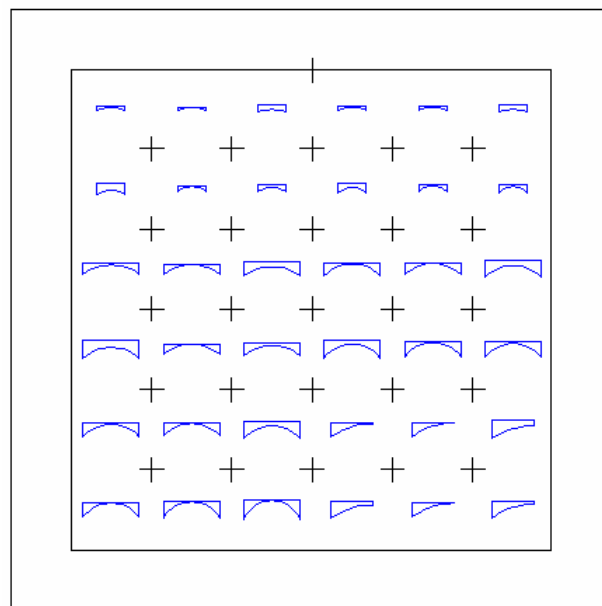


Fig. 4-5. Schematic of contour mask for fabricating lenticular-lenses.

4.3 Fabrication Stability and Lens Quality

Several variables were considered for obtaining the quality and stability of fabricating lenticular-lenses arrays by excimer laser micromachining system.

4.3.1 Energy Stability

The excimer laser has been detected continuously for the 4 weeks by energy detector as shown in Fig. 4-6. The detected energy is the amount of output before emerging through the condensed lens. Because the detected energy is the reference for us to see the trend of laser stability, the unit between detected energy and input energy are not important. The relationship between input energy and detected energy is linear as shown in Fig. 4-6.

During the fabrication period, the maximum input energy can be obtained was found to be 240 mJ. The detected energy shows the input energy is similar for each week, except the 2nd week was lower. The lower laser energy is due to low gas pressure and can be avoid by changing the KrF gas. In addition, each shot of excimer laser has some tolerance. The deviation, which is defined as the percentage of variance energy different from average laser shot energy, of laser shot in each week has also been evaluated as shown in Fig. 4-7. While input energy is higher, deviation becomes smaller. Deviations are in the range of 4 ~ 7 % of detected energy for these 4 weeks. As the result, the energy stability of excimer laser can be relied on with keeping an eye on the level of gas pressure.

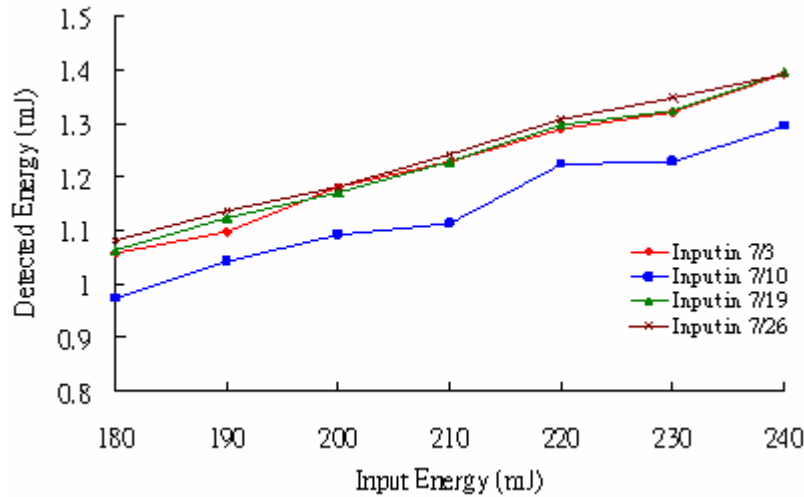


Fig. 4-6. Excimer laser energy for 4 weeks continuously.

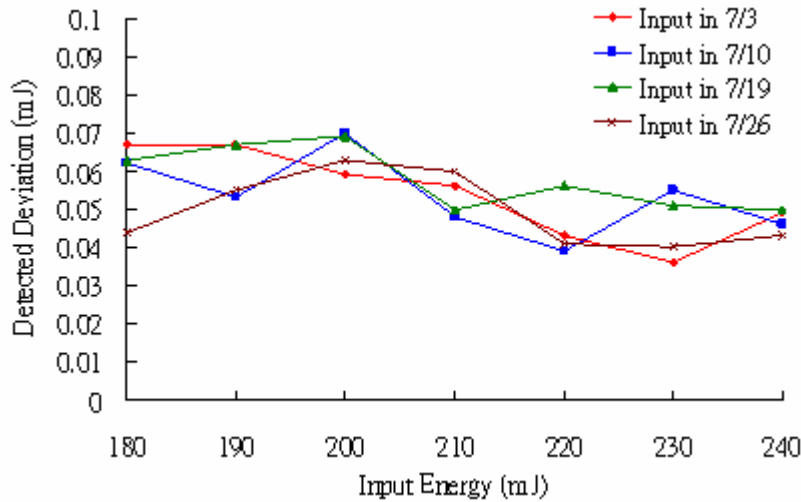


Fig. 4-7. Deviation of laser shot for each week.

4.3.2 Lens Radius with Laser Energy

Fewer variables mean fewer dependents which have brought more convenient in further investigation. We have attempted to convert laser energy includes its input energy and attenuation to the independent constant. In addition, lens radius does not change a lot when laser energy is about 200 mJ as shown in Fig. 4-8. As set up the maximum laser energy to be 240 mJ, the attenuation coefficient could be chosen as 0.8 to be more flexible for further adjustment. In this experiment, the laser energy

after attenuation is 192 mJ, laser energy output of each shot seems to be stable at this level. Hence, the variables of fabrication considerations have reduced to laser penetration rate and stage feeding rate.

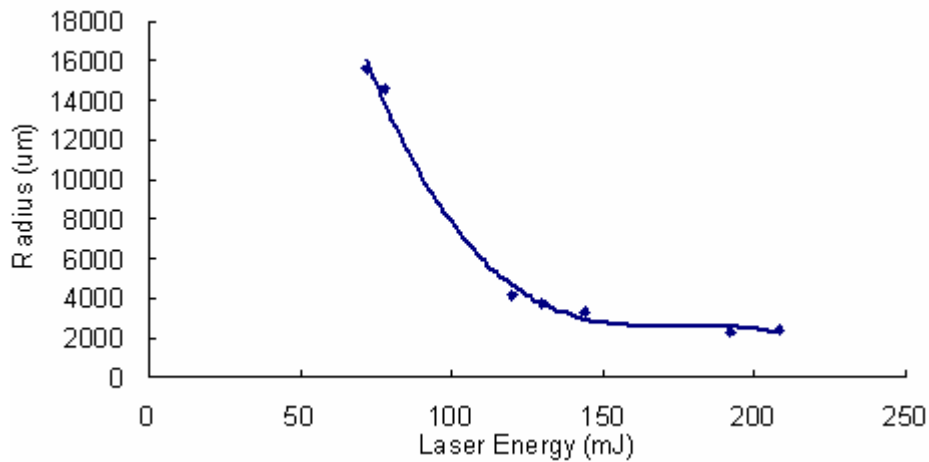


Fig. 4-8. Lens radius with laser energy.

4.3.3 Lens Radius with Laser Penetration Rate

Penetration rate is inversely proportional to the fabricated lens radius as shown in Fig. 4-9. Higher penetration rate will have smaller lens radius, rougher lens surface and thinner the substrate. According to the trend line, it seems the number approaching 18 Hz is preferable to the proposed design. However, when the penetration rate reaches 18 Hz, the substrate becomes very thin for the small lens radius in our contour mask design. The thinnest point may break through the substrate. Therefore, the range of penetration rate has to be as small as possible, at least should be less than 18 Hz, in the experiment. Thus, we have to use the other variable, such as stage feeding rate to cover the insufficient of lens curvature.

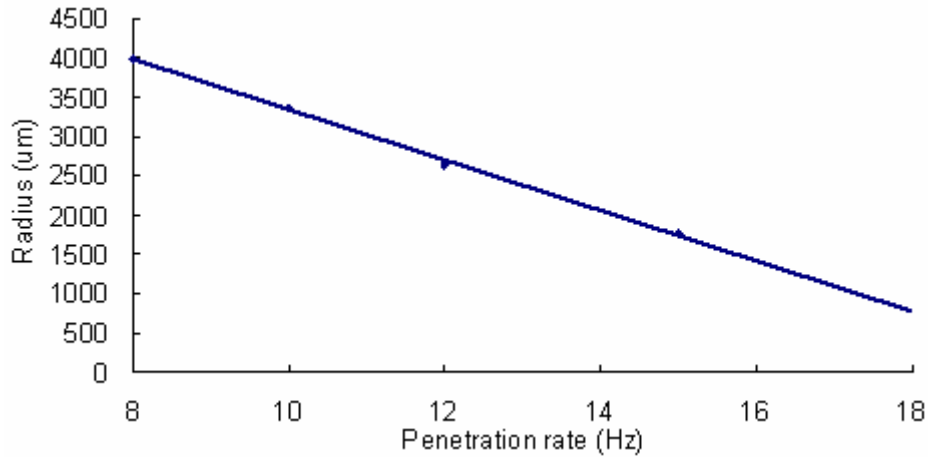


Fig. 4-9. Lens radius with laser penetration rate.

4.3.4 Lens Radius with Stage Feeding Rate

When stage feeding rate is smaller than 2 mm/min., the radius of fabricated lens is sensitive to the stage feeding rate as shown in Fig. 4-10. In order to obtain the expected radius, it has to complement with laser penetration rate. Due to the target of our lens design, which is between 600 um and 800 um, the stage feeding rate has to be less than 3 mm/min. The lower stage feeding rate helps in improving the surface smooth. Nevertheless, lower the stage feeding rate increases the fabrication period, for example, the stage feeding rate of 0.5 mm/min. needs double time period of 1 mm/min. This is a trade off in the fabrication consideration. Thus, in this experiment, stage feeding rate is chosen from 1 mm/min to 3 mm/min.

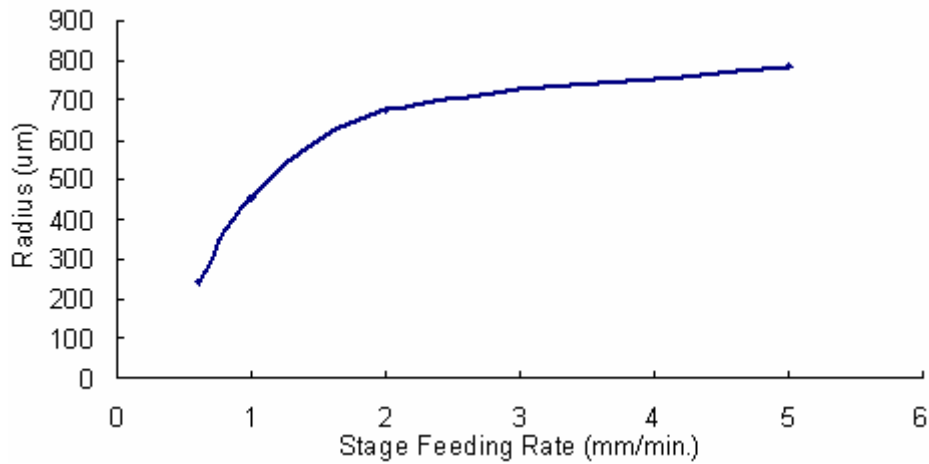


Fig. 4-10. Lens radius with stage feeding rate.

4.4 Fabrication Tolerances

The deviations in the fabrication are almost incapable to avoid totally. The possible errors of fabricating by Excimer laser micromachining system are dual curvatures in single lens and lens gap in between lenses. In order to obtain the desired functions, the effects of inaccurate fabricated samples have to be discovered and simulated.

4.4.1 Dual Curvatures Effect

Dual curvatures effect maybe occurred when the excimer laser is not uniformly distributed in the projecting area. If the left or right portion of projecting area has larger amount of laser energy, the resulted lens radius will be smaller. The schematic of singular curvature and dual curvatures lens structures is shown in Fig. 4-11.

Since one portion of lens is taller than another, some light will be blocked by the taller portion. The simulated results of varies pairs of dual curvatures in single lens are shown in Fig. 4-12. While the deviations of lens radius between left and right

portions are similar, the resulted viewing angles are same as the desired function. Moreover, until the deviations reached 50 μm as shown in Fig. 4-12 (d), some light path may be blocked to result narrower viewing angle. The study shows the uncertainty of left and right portions in single lens has to be small as possible, thus, the desired viewing angles can be obtained.

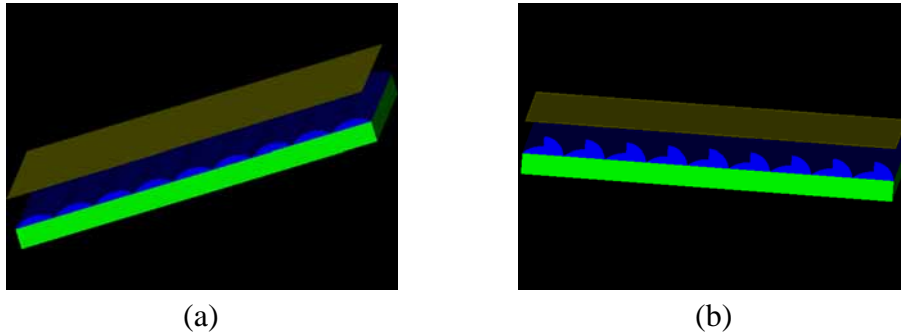


Fig. 4-11. Schematics of (a) singular curvature and (b) dual curvatures lens structures.

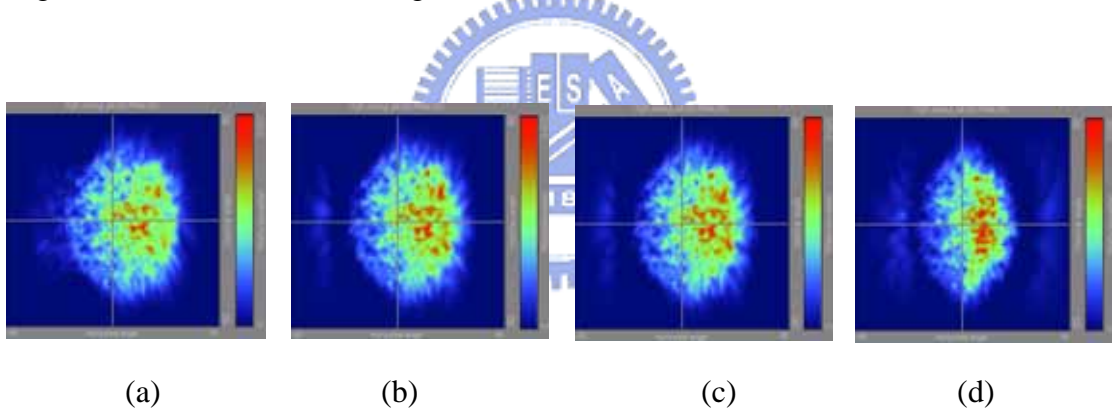


Fig. 4-12. Simulated results of half lens with radius of 150 μm and another half with radius (a) 200 μm , (b) 150 μm , (c) 140 μm and (d) 100 μm .

4.4.2 Lens Gap Effect

In the Excimer laser micromachining system, the lenticular-lenses are fabricated one by one. There may be the gaps in between the lenses as shown in Fig. 4-13. Since the fabricated substrate is colorless, the undirected light will pass through and then mix up with expected light strips. Hence, the resulted images may be blurred due to light interference. The 3D functional layer will lose its functioning ability. Therefore,

the lens design may need to seek for continued lenses and avoid the gaps in between lenses.

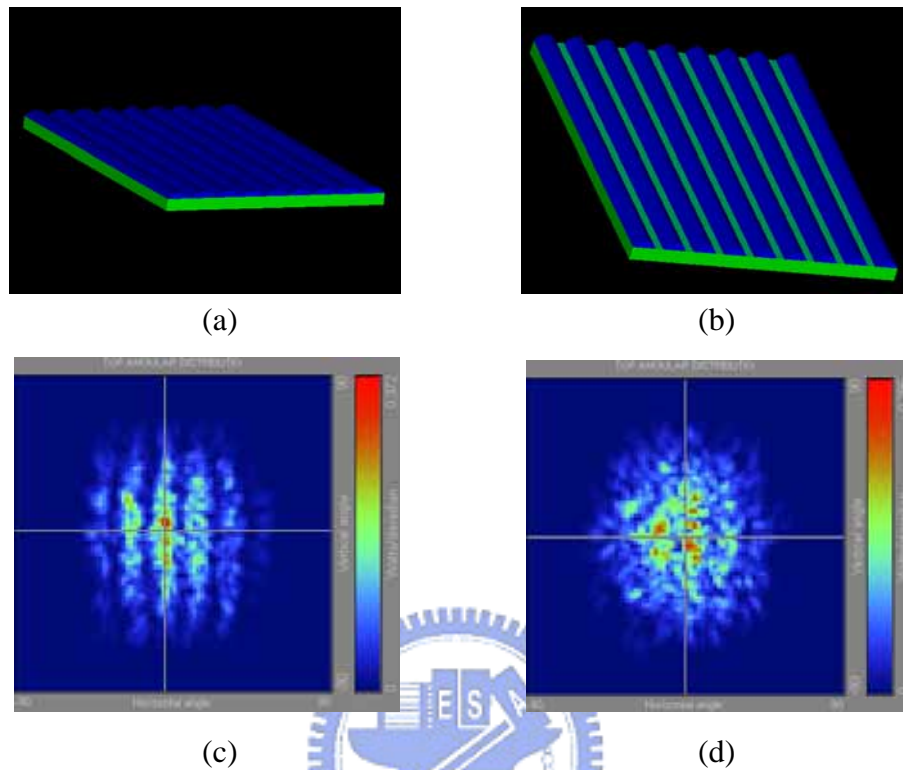


Fig. 4-13. Schematics of lens structures with (a) no gap and (b) gaps, and their respected simulated results.

4.5 Experiments

The proposed micro-optical elements were fabricated by using Excimer laser micromachining system with contour mask at Instrument Technology Research Center (ITRC) to fabricate. The laser system used is an Excitech 7000 series excimer laser workstation as shown in Fig. 4-14.



Fig. 4-14. Appearances of Excitech7000.

Energy of excimer laser, number of micromachining pulses so called # of shot, and laser repeat rate can be precisely controlled to our need. We chose the projection system with 10x because the higher demagnification increases the resolution of the microoptical elements fabricated by using contour mask, i.e. the minimum pixel size on the elements shrink. NA is 0.2. The material of work is a PC polymer (polycarbonate) of the thickness 0.5 μm (purchased from Goodfellow).

The micromachining parameters and target sample parameters are shown in Tables 4-1 and 4-2. The outlook of target sample is shown in Fig. 4-15.

After excimer laser micromachining, the radius of fabricated lenses and its angular distribution of light intensity are measured by using Zygo's optical interferometer as shown in Fig. 4-16 and Conoscopic system as shown in Fig. 4-17.

Table 4-1. Micromachining parameters.

Parameters	Values range
Energy	240 mJ/pulse
Attenuation	0.8
Laser penetration rate	10 ~ 18 Hz
Stage feeding rate	1 ~ 3 mm/min.

Table 4-2. Fabrication targets for the lenticular-lenses arrays.

Parameters	3D function	Double-screen function
Ra (Maximum Roughness)	$\leq 1.0 \text{ um}$	$\leq 1.0 \text{ um}$
C (Lens radius)	$650 \pm 50 \text{ um}$	$800 \pm 50 \text{ um}$
X (Lens pitch)	594 um	1188 um
D (Single lens height)	66 um	264 um
H (Substrate thickness)	$\leq 500 \text{ um}$	$\leq 500 \text{ um}$
W (Substrate width)	17426 um	21780 um
L (Substrate length)	21780 um	17426 um

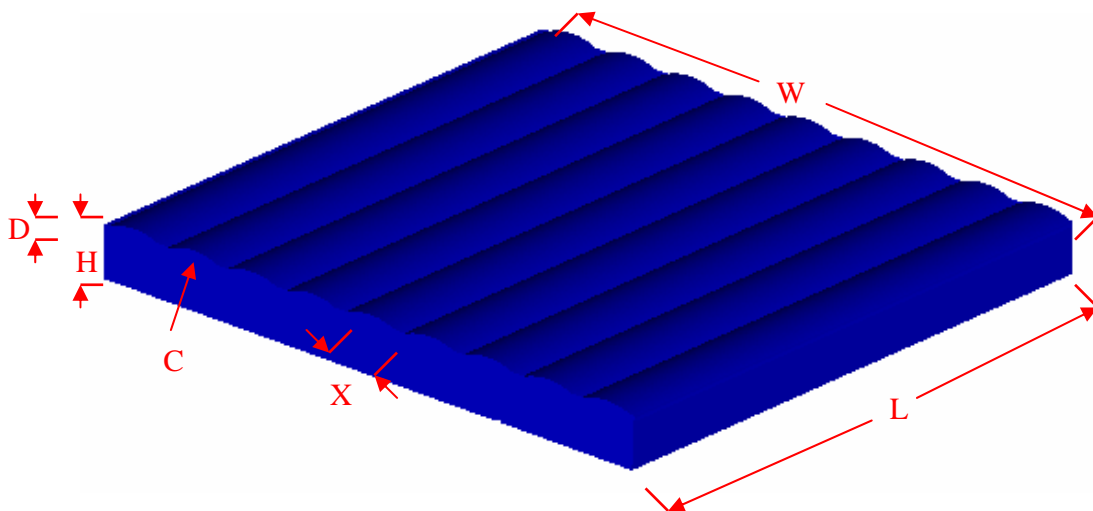


Fig. 4-15. Outlook of a set of lenticular-lenses to be fabricated.



Fig. 4-16. Appearances of Zygo's optical interferometer.



Fig. 4-17. Appearances of ELDIM EZContrast 160 measurement system.

4.6 Experimental Results and Discussions

The experiment is taken based on verifying the simulated results with the reality on lens radius and viewing angle for both functions.

4.6.1 Lens Radius

The sample of lenticular-lenses-based micro-optical structure with the diagonal of 0.54 inch, as shown in Fig. 4-18, is mainly fabricated by Excimer laser micromachining system. The lenticular-lens pitch and length are 3.6 mm and 11 mm, respectively. By utilizing Zygo's interferometer to inspect the fabricated substrate, the results of lens thick and lens half width, as shown in Fig. 4-19, can be used with equation 3-7 to calculate the lens radius as shown in Table 4-3.

From the experimental results, we can find that trial 3 and trail 13 are close to the design for double-screen and 3D functions, respectively. In addition, by using the similar settings as trails 2 and 4, excimer laser has fabricated the lenses twice with similar output results within ± 50 μm . The smooth of surface is less than 1 μm which is acceptable for our design. In the other words, the excimer laser has high possibility of reproducing the lenses. Comparing to double-screen function, 3D function layer is more difficult and needs more time to fabricate due to its smaller pitches dimensions. Nevertheless, 3D and double-screen function layers can be fabricated by excimer laser with the laser energy equals 240 mJ, attenuation 0.8 and stage feeding rate 1 mm/min. The only variable is penetration rate which for 3D and double-screen function layers are 10 Hz and 15 Hz, respectively.

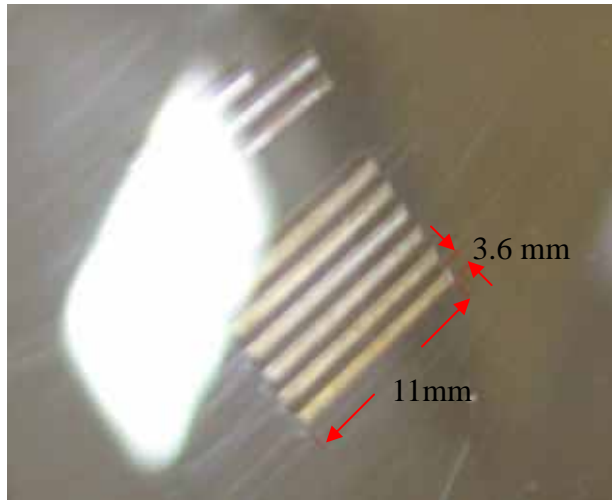


Fig. 4-18. Photograph of sample fabricated lenticular-lens for double-screen function.

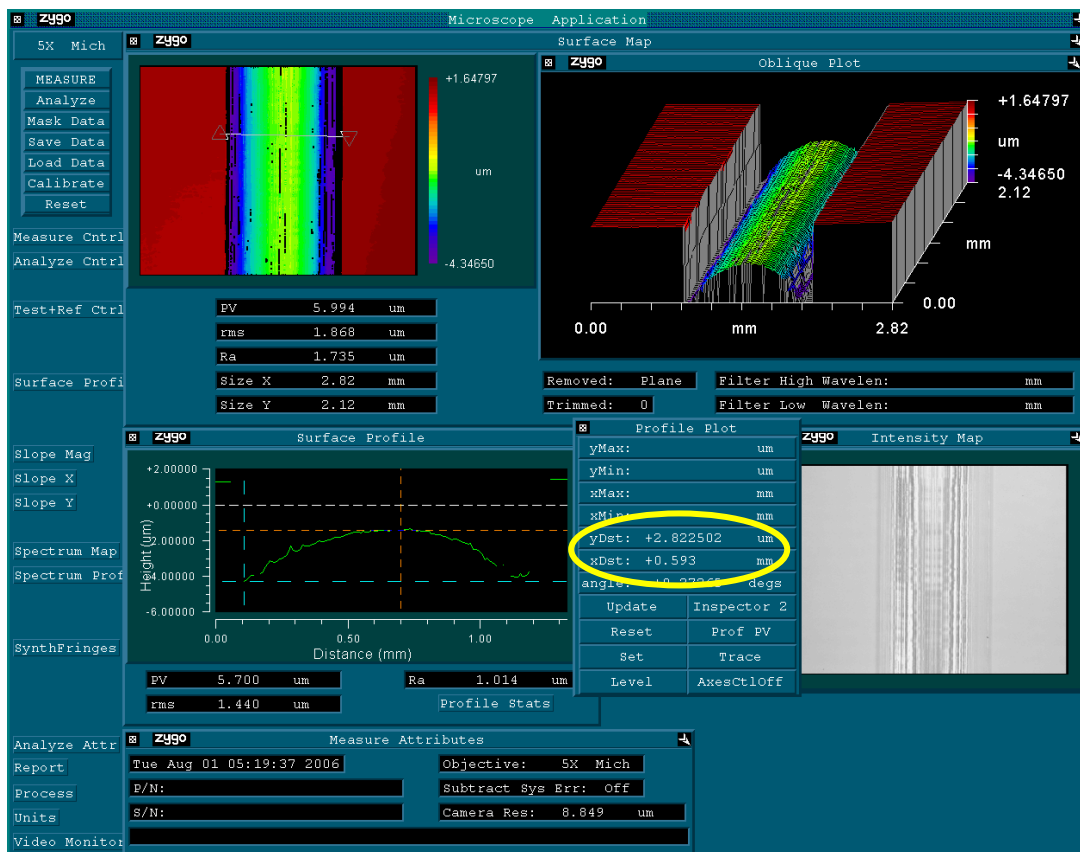


Fig. 4-19. Measured results of Zygo's interferometer.

Table 4-3. Fabrication parameters and resultant lenses radii of each trail.

Double-screen Function								
Trial #	Fabrication parameters				Measured results			Calculated
	Energy (mJ)	Atten.	Pen. rate (Hz)	Feed. rate (mm/min)	Roughness (um)	Half lens pitch (um)	Lens thickness (um)	Radius (um)
1	240	0.8	18	1	0.564	131	3.55	606
2	240	0.8	15	1	0.268	149	4.59	607
3	240	0.8	15	1	0.723	109	2.32	642
4	240	0.8	15	1	0.255	53	0.52	677
3D Function								
Trial #	Fabrication parameters				Measured results			Calculated
	Energy (mJ)	Atten.	Pen. rate (Hz)	Feed. rate (mm/min)	Roughness (um)	Half lens pitch (um)	Lens thickness (um)	Radius (um)
11	240	0.8	12	1	0.625	319	20.64	627
12	240	0.8	15	2	0.505	100	1.86	673
13	240	0.8	10	1	0.757	122	2.39	779

4.6.2 Viewing Angle for 3D and Double-screen Functions

The simulation for the top screen of the double-screen function yields the viewing angles of $-45^{\circ} \sim 45^{\circ}$ and $-5^{\circ} \sim 40^{\circ}$ in horizontal and vertical directions, respectively. After testing the sample by Conoscopic System, the measured viewing angles are $-60^{\circ} \sim 60^{\circ}$ and $-10^{\circ} \sim 40^{\circ}$ in the horizontal and vertical directions, respectively. The simulated and experimental results for double-screen function are compared in Fig. 4-20. The experimental results show the wider viewing angles in the horizontal direction. Since double-screen function used to direct the light paths in vertical directions, the wider of horizontal direction does not affect the results.

The experimental result of 3D function is wider than the simulated result, but they have the similar feature, 3 viewing screens. There are several possible reasons of having different magnitudes with the similar trend. The obviously reason is that the lambertian light's incident angle of Conoscopic System is larger than the settings of the simulation. Moreover, the coordinate axes of the simulation software and measuring

system are different. Simulation software has coordinate axes in X and Y. The Conoscopic System has the axes in Phi and Theta. Since the Phi and Theta can project on X and Y axes, the relationship between both coordinates' measured results will have similar trend. The results show similar tendency of using different coordinate systems, but the magnitude of the results will not be the same values. Furthermore, the other reason may be the difficulty of alignment for the small dimensional objects. Due to the necessary of blocking the opponent directional light, the barrier has to locate at precise position and only let the designated directional light passes through. Due to the tiny aligning point and colorless substrate, there are some crosstalk happened.

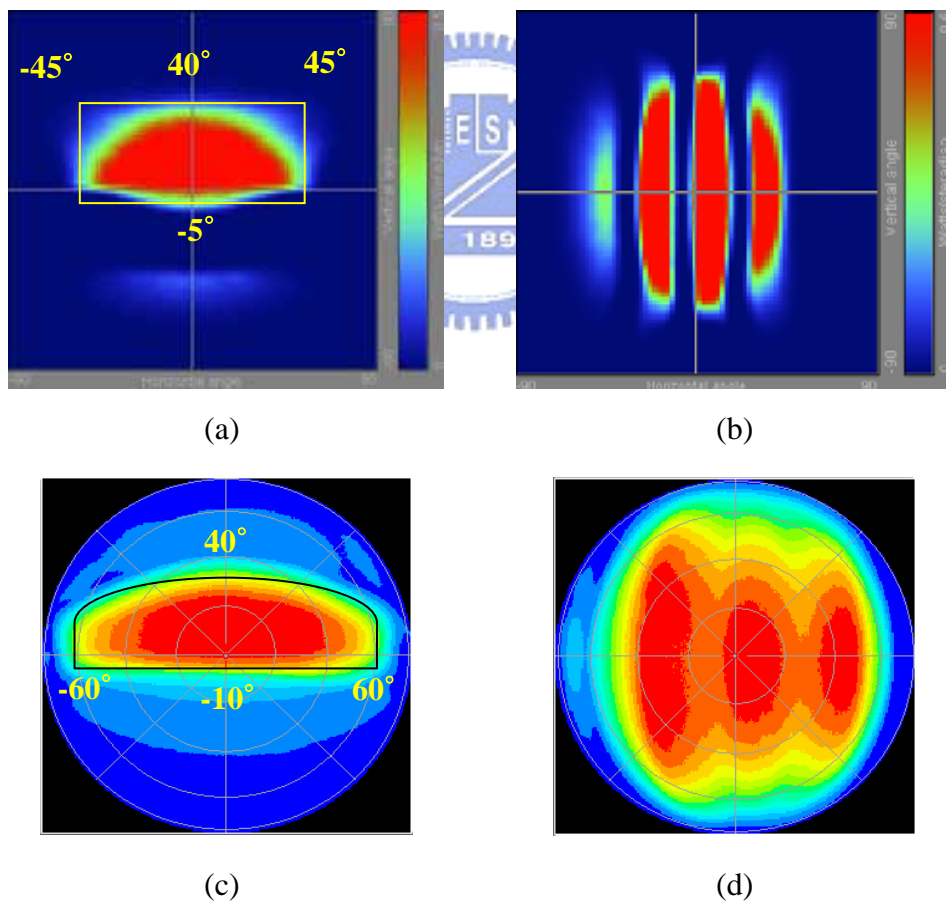


Fig. 4-20. Angular distributions of simulated results on (a) top screen of double-screen function and (b) right eye of 3D function, and the experimental results on (c) top screen of double-screen function and (d) right eye of 3D function.

4.7 Summary

A prototype of micro-optical structure for 3D and double-screen functions was fabricated by the excimer laser micromachining system. The fabrication parameters, such as laser energy, attenuation, penetration rate and stage feeding rate are found to be 240 mJ/pulse, 0.8, 10 Hz ~18 Hz and 1 mm/min. ~ 2 mm/min., respectively. As the result, the lens radius can be estimated from the measured half lens pitch and lens thickness. The radii of fabricated lenticular-lenses for 3D and double-screen functions are within the tolerances of design values, 800 ± 50 μm and 650 ± 50 μm , respectively. Moreover, due to the difficulty of aligning colorless samples during the measurement, the measured viewing angles for both functions are wider than the simulated results. The trend of occurring light strips, however, is similar in both cases. Thus, the experimental results proof the possibility of fabricating the lenticular-lenses-based micro-optical structure by excimer laser micromachining system.



Chapter 5

Mechanism of Converting an Ordinary Flat Panel Display to 3D Double-screen Display

5.1 Introduction

After the optical system has designed to generate two screens of 3D images and the micro-optical structure has fabricated by excimer laser, the next import factor of building up the 3D double-screen display is to organize the components and input the suitable images to feet the hardware. If the alignment between the fabricated lenticular-lenses layers and ordinary panel has noticeable slanted angel, moiré patterns may appear. Moreover, even if the components are aligning precisely, observers still can not view the desired images by the display system with the unmatched images' inputting. Therefore, the mechanisms include attaching micro-optical structure on a flat panel and processing digital images are necessary to be studied.

5.2 Algorithm of Digital Image Process

The purpose of proposed micro-optical structure is to direct light paths from color filter to the desired viewing screens. In order to yield exhaustive pictures in all viewing screens, pixels have to be grouped as row-based or column-based to provide the images for different directions. Hence, the ordinary images have to be modified in order to generate the correct images. The images transformation system is, therefore, needed.

3D double-screen images algorithm, as shown in Figs. 5-1 and 5-2, is developed from utilizing digital image process technique. From the implantation, the images are split and recombined to form a combination image for each eye or direction as shown in Fig. 5-3. When the 3D image is needed, the left and right eyes images are combined pixel by pixel as shown in Fig. 5-4. Similarly, double-screen images are the combination of bottom screen and top screen images as shown in Fig. 5-5. Thus, the algorithm of generating 3D and double-screen images step by step yields satisfactory 3D double-screen images.

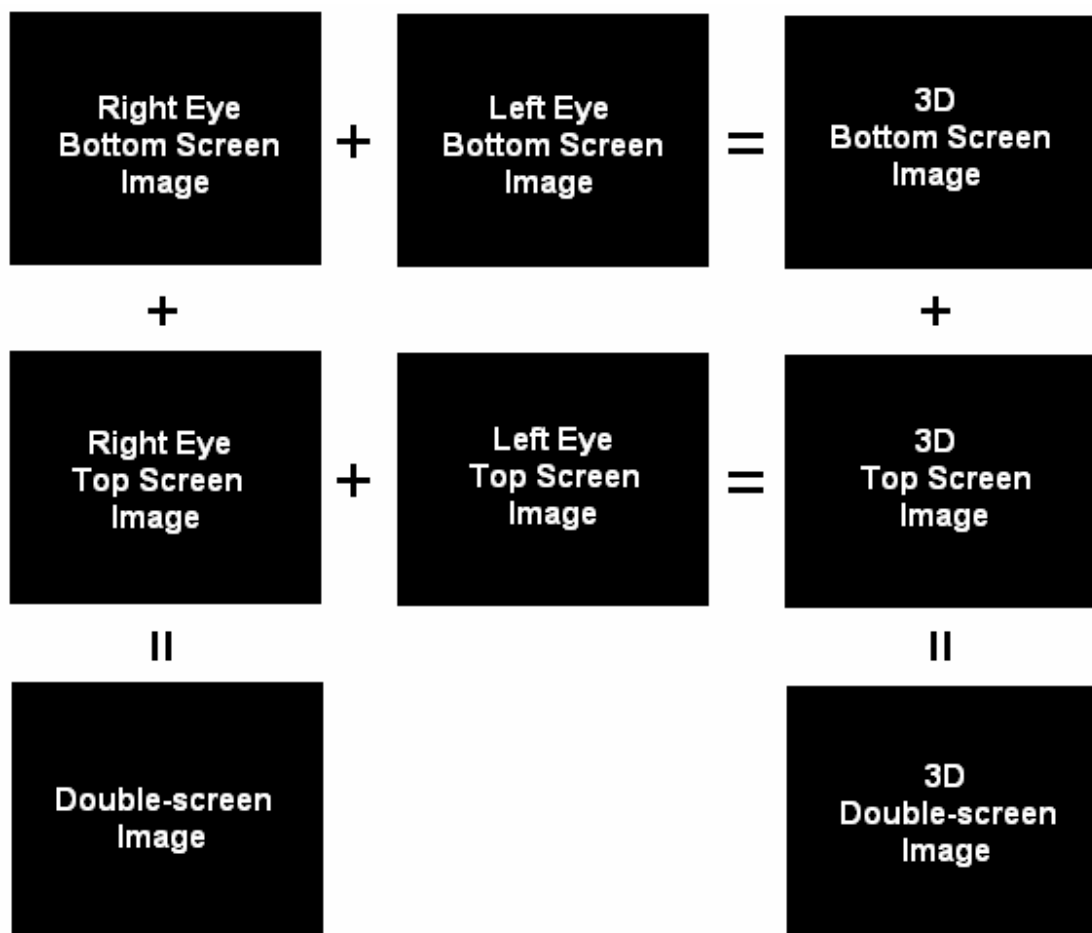


Fig. 5-1. Concept map of 3D double-screen images algorithm.

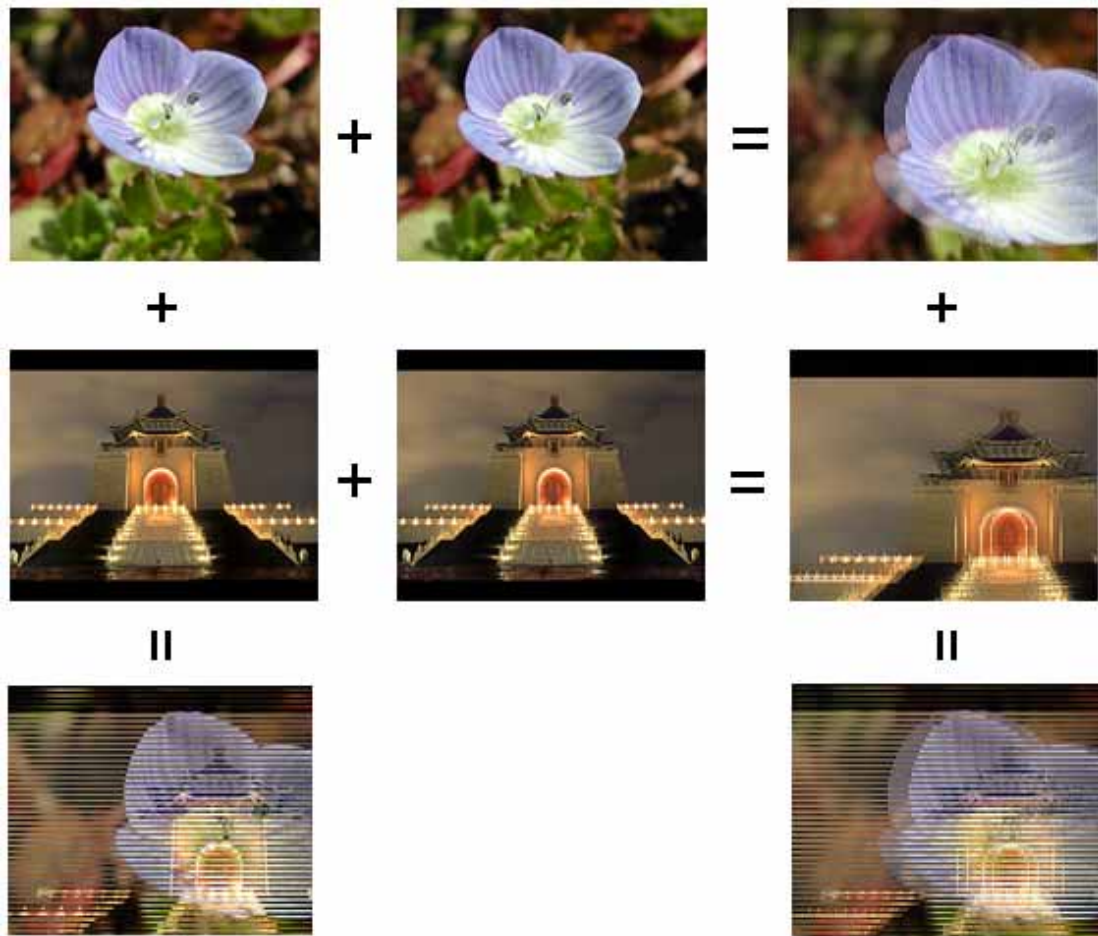


Fig. 5-2. Real images map of 3D double-screen images algorithm.

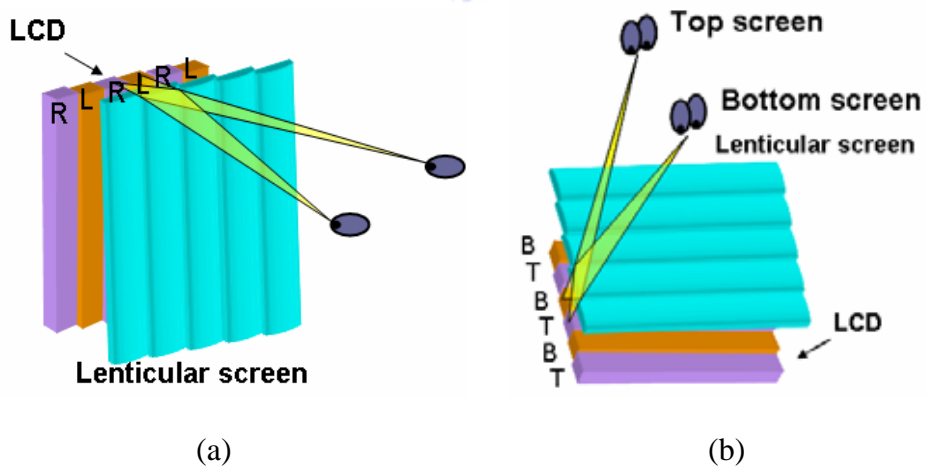


Fig. 5-3. The schematic outlook with (a) left and right pixels for 3D function and (b) top and bottom pixels for double-screen function.

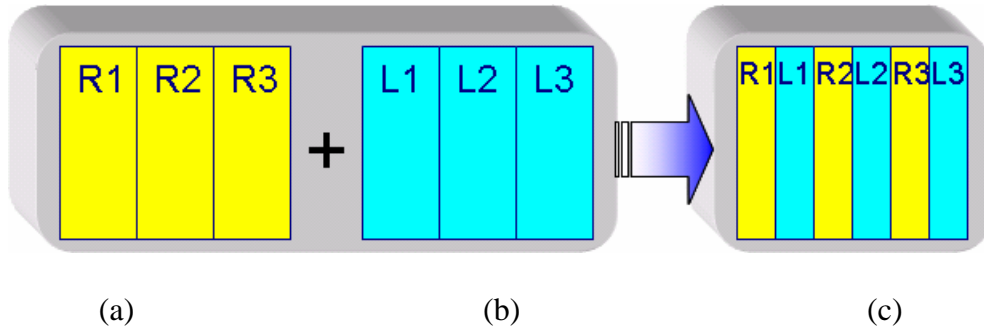


Fig. 5-4. (a) Right eye [R], (b) left eye [L] and (c) 3D [R+L] images.

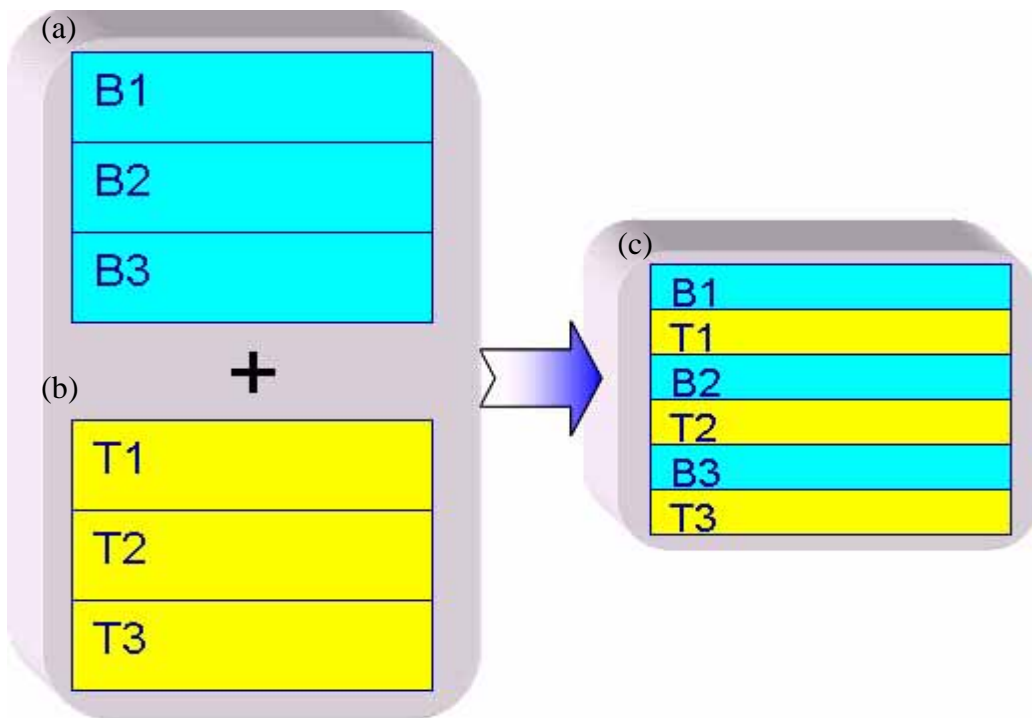


Fig. 5-5. (a) Bottom screen [B], (b) top screen [T] and (c) double-screen [B+T] images.

5.3 Alignment of Micro-optical Structure

In order to have the 3D and double-screen images, the designed micro-optical structure, which consists 3D and double-screen functional layers, has to be pasted on the panel. Due the pitches for pixels' and lenses' are in very small dimensions, human eyes would have difficulty on perceiving and aligning them properly. Therefore, the viewing angles caused by the alignment effects have to be discovered.

5.3.1 Aliasing

By utilizing simulation software as the tool in finding the causes for the alignment deviations in horizontal or vertical directions, the shift of resulted viewing angle range is clearly presented and easily compared. When the lenticular-lenses and pixels are aligned in the designed position as shown in Fig. 5-6 (d), the simulated result shows the angular distribution of light intensity has viewing angles from approximately 0° to 30° as shown in Fig. 5-6 (a). With this resulted viewing angle range, the structure favors in generating right directional image of double-screen function. In addition, by moving the lens layer to the left of the color filter little by little, the resulted viewing angle range will shift from right side to left side and become smaller and smaller as shown in Figs. 5-6 (a), (b) and (c). The original design of double-screen function will, therefore, lose its capability.

The changes of viewing angle ranges depend on the alignment deviations. While the lenticular-lenses and pixels are aligned with 0.1 mm tolerance as shown in Fig. 5-6 (e), two almost equivalent portions of viewing angle regions appeared at left and right sides. After that, the right directional image becomes appearing at left side when alignment tolerance is between 0.1 mm and 0.2 mm. If tolerance is bigger than 0.2 mm as shown in Fig. 5-6 (f), the resulted viewing angle range become two portions which are -36° to -10.5° and 21° to 43° for left and right spots, respectively, as shown in Fig. 5-6 (c). Thus, the lenticular-lens is no longer to precisely direct the light into the desiderative region in the misaligned situations. The double-screen function, therefore, may not exist any more. Consequently, alignment between the lenses and pixels is the key to maintain the power of both functions in generating 3D and double-screen images.

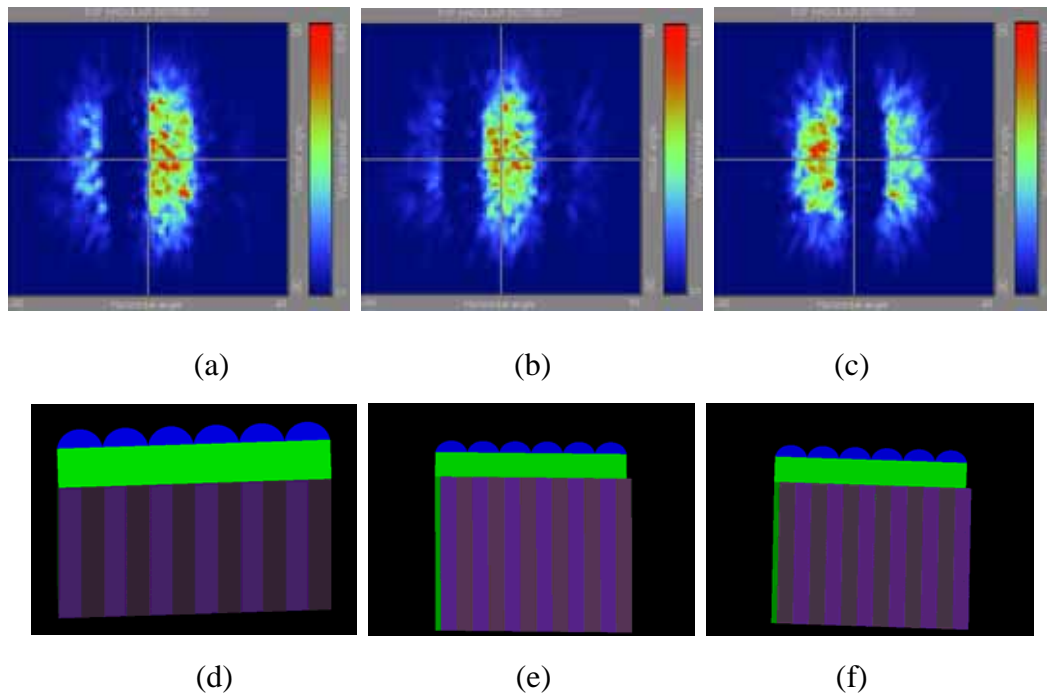


Fig. 5-6. Angular distributions of the double-screen function for (a) aligned well, (b) 0.1 mm tolerance and (c) 0.2 mm tolerance with their respective outlooks (d), (e) and (f).

5.3.2 Moiré Patterns



Moiré pattern is caused by interference with two or more periodic structures as shown in Fig. 5-7 [21]. In the proposed structure, moiré patterns occurred when the substrates are attached with tilt angle. Each layer of the lenticular-lens arrays should be perpendicular to each other which means one should align horizontally to the panel pixels, and another should align vertically to the panel pixels. If the tilt angle is approaching to 45° , the moiré patterns will be shown more clearly. However, moiré patterns are minimized when the tilt angles between each layer are 0° and 90° . Thus, one of the solutions to avoid the moiré patterns is to align each layer on the panel properly in desired angles, such as 0° and 90° for 3D and double-screen functions.

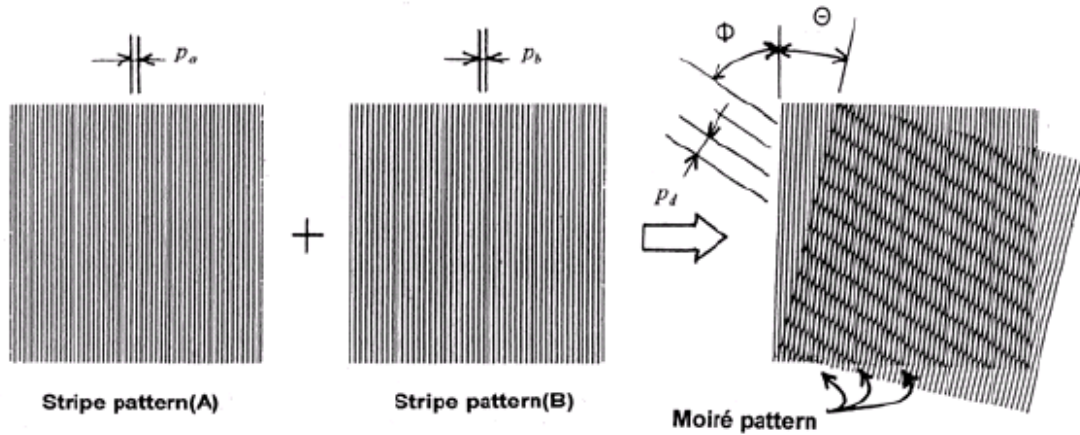


Fig. 5-7. Cause of moiré patterns.

5.4 Experimental Results

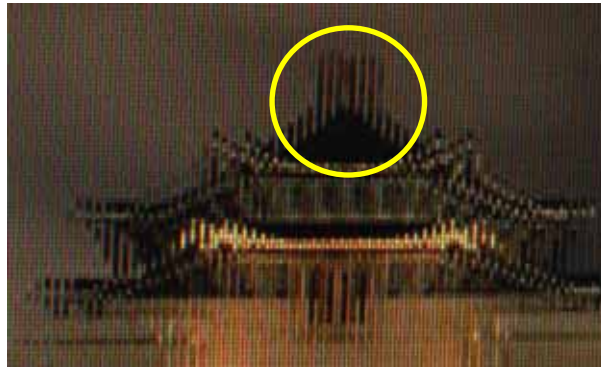
To verify the reality of the proposed structure, the demonstrations are processed with several 3D and double-screen images. The proposed micro-optical structure which comprises two sets of lenticular-lenses is designed to stick-on an ordinary panel to generate the expected images. By pasting a set of lenticular-lens on the panel which has 3D image modified, as shown in Fig. 5-8 (a), the realistic 3D images can be perceived as shown in the circle of Figs. 5-8 (b) and (c). Within the attached region (the circle region), the image of a roof is clearly shown up, not like the other areas are shown blurred images. Furthermore, by implanting black & white strips instead of processed images as shown in Figs. 5-8 (d) and (e), the proposed structure has successfully generate black and white images for left and right eyes, respectively. The simulated results show the validation of the model design.

By replacing the other set of lenticular-lenses which designed for double-screen function on the panel, two different images can be generated as shown in Fig. 5-9 (a). The observers are proposed to view the roof in the top screen while perceiving the petal

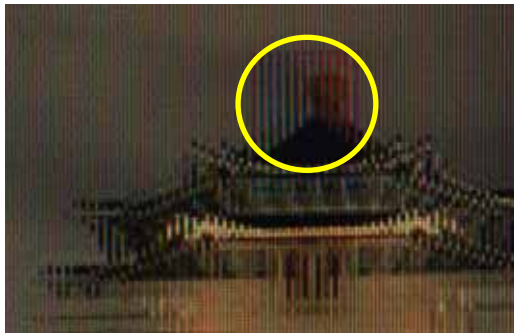
in the bottom screen. Moreover, the double-screen function can still operate by replacing the processed images with black & white strips as shown in Fig. 5-9 (b). The results of inputting black & white images are similar with inputting the processed images. The experiment shows the double-screen functioning ability of the proposed functional layer. Thus, the possibility of proposed micro-optical structure splitting a single screen image to two different screens images has verified.

With adding the 3D functional layer on the top of double-screen layer, the display yields 3D double-screen images. The left and right eye's images of both screens are shown in Fig. 5-10. The adopted system utilizes a LCD, which consists of the proposed structure pasted on and a mirror representing the top and bottom screens, can generate dual 3D images simultaneously.

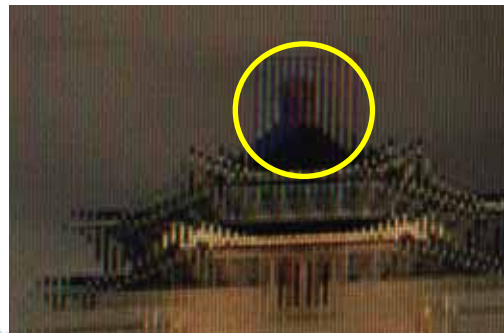




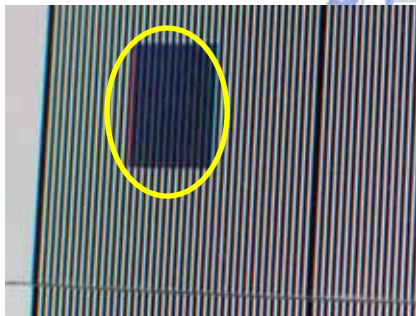
(a)



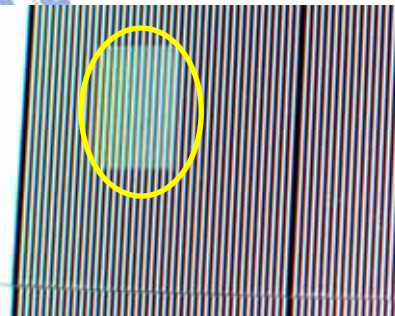
(b)



(c)

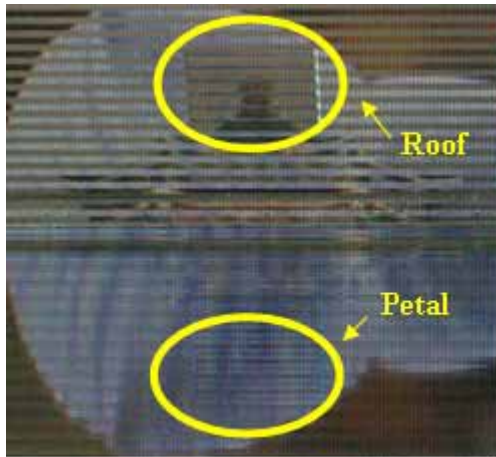


(d)

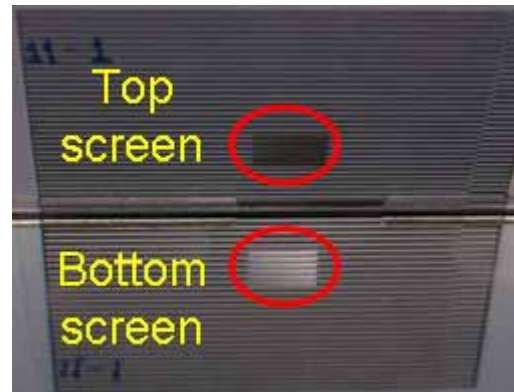


(e)

Fig. 5-8. Demonstrated results of (a) image without, 3D images of (b) left eye and (c) right eye, and black & white images of (d) left eye and (e) right eye with attaching micro-optical structure on the panel.

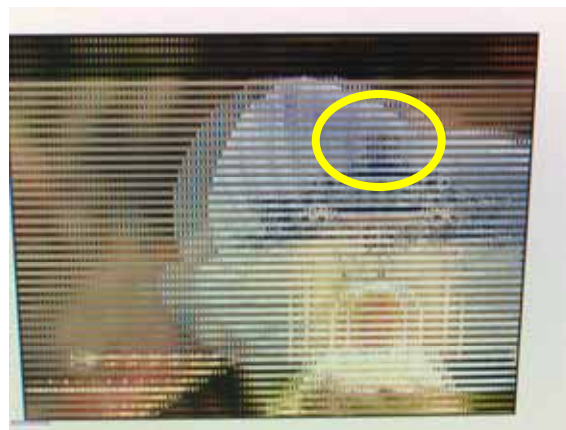


(a)



(b)

Fig. 5-9. Demonstrated result of the panel with attaching another set of lenticular-lenses (top screen's circle area) for (a) processed images and (b) white & black strips for double-screen function.



(a)



(b)

(c)

Fig. 5-10. Demonstrated results of (a) without attaching micro-optical structure's image and with attaching for (b) left and (c) right eye's 3D double-screen images.

5.5 Discussions

The images of the demonstration were taken by the digital camera without any other modification. Due to the limitation of the camera's performance and light reflection, there are some parts of the lenses areas became a little reddish in the photographs. Besides, the proposed 3D function is based on parallax, thus, the observers are receiving the right/left eye images to the right/left eye. After that, the 3D images will be reconstructed in human's brain. Due to the restriction of the ordinary digital camera on photographing multiple images simultaneously, the images for each eye have to be taken separately. Because the objects in both images are presented evidently, the micro-optical structure can be defined as possessing splitting light ability. In addition, the left eye and right eye images are about 6.5 cm horizontally. Both eyes images can be recombined to be the 3D images in the human's brain.

For double-screen function, the performance of demonstrated images on the ordinary panel may seem differently with our expectation. Some unwanted black strips are occurred by misalignment. Misalignment includes the distance between with color filter and tilt angle of the micro-optical structure. When the thickness of the substrate is insufficient to our design, the light path becomes shorter than the expected. Hence, some portions of images may not get enough light and may yield the black strips. However, the unwanted strips can be eliminated by adding the gap between the substrate and the panel or increasing the thickness of the substrate itself.

Since the demonstrations of 3D and double-screen functions match the simulated results, a 3D double-screen display based on the combination of both lenticular-lenses sets should generate two 3D full-sized images as well. The further investigation will start with improving the image quality by eliminating the unwanted black strips. After

optimizing the performance for each function, the materialization of optimized 3D double screens display can be fabricated to perform two excellent realistic scenes simultaneously in near future.

5.6 Summary

The mechanism of transforming the ordinary displays to 3D double-screen displays has developed after studying both software and hardware. The 3D double-screen algorithm utilized digital images processing techniques, which includes splitting and recombining pixels to form 3D, double-screen and 3D double-screen functional images. After software is ready to use, the alignment issues, such as aliasing and moiré patterns are studied. The major solution is to align properly in horizontal, vertical and enclosing directions with sufficient substrate thickness. After that, by pasting the fabricated lenticular-lens-based optical system on a flat panel display, the 3D double-screen images could be generated in the display. The results demonstrated the proposed architecture has high potential of obtaining the 3D and double-screen functions in a flat panel display.

Chapter 6

Conclusions and Future Works

6.1 Conclusions

An optical system for novel 3D double-screen display has been investigated and verified. The system comprises a mirror and a lenticular-based micro-optical structure to generate dual full-sized 3D images. The prototype of double-screen function is based on increasing the pitch size of 3D function's lenticular-lens by rotating the layout of color filter from portrait to landscape. By combining both sets of lenticular-lenses in cross-over, double-screen and 3D functions can be generated simultaneously. In addition, the image crosstalk has minimized by the optimization of micro-optical structure, including substrate thickness, material refraction index, lens pitch and lens radius. Two full-screen-sized 3D images have been successfully simulated with resulting the viewing angles around $-35^{\circ} \sim 35^{\circ}$ and $\pm 5^{\circ} \sim \pm 40^{\circ}$ in the horizontal and vertical directions, respectively.

The lenticular screens for 3D and double-screen functions were fabricated by Excimer laser micromachining system. The radii of fabricated lenticular-lenses for 3D and double-screen functions are within the tolerances of design values, 800 ± 50 μm and 650 ± 50 μm , respectively. The trends of light strips for simulated and experimental results are similar. Hence, the experiments show the possibility of having the designed model to be fabricated by using this manufacturing technology.

The mechanism of digital images process between the ordinary and 3D double-screen images was established. By pasting the proposed lenticular-lens-based

optical system on a flat panel display, the 3D double-screen images could be generated. The demonstrations show the high possibility of transforming the flat panel display to obtain the 3D and double-screen functions in a single display system by using the proposed novel architecture.

6.2 Features

There are several features of the proposed system. First, there are minimum structures needed. The required components are the proposed micro-optical structure, a flat panel and a mirror. By including these simple components, the ordinary flat panel display could be easily converted to 3D double-screen display. Moreover, the second advantage is simple fabrication process. The proposed micro-optical structure can be easily and economically fabricated in large amounts by utilizing direct writing method, Excimer laser micromachining system. Finally, the most attraction of the design is to provide the ability of viewing two full-screen sized 3D images simultaneously. By adjusting the numbers of functional layers, the display can also show either 3D, double-screen or 3D double-screen images to fit in with observers' desires.

6.3 Future Works

The study on 3D double-screen display has provided the know-how on utilizing single panel to display multi-screen images. Since the fundamental knowledge of designing the lenticular-lens-based optical system has been studied, the single panel 3D multi-screen display could be further developed by expending the research in the following categories, such as developing an advanced algorithm for processing the

realistic multi-screen dynamic images, replacing with advanced substrate materials for obtaining the required refraction indexes of 3D and multi-screen functions, inserting liquid crystal into the lenticular-lenses for the capability of switching functions, fabricating two layers of lenticular-lenses in a single sheet for thinner the attached structure, and implanting time-multiplexed method for higher resolutions on 3D images. Thus, the single panel 3D multi-screen display with switchable function can generate high resolution, realistic and multi-screen full-sized images. With the further improvement of the converting mechanism, the ordinary flat panel displays will have high potential to become the single panel 3D multi-screen displays.



Reference

- [1] J. A. Castellano, "Handbook of display technology", Academic Press, San Diego (1992).
- [2] T. Ito, "Foundations of the 3D television", NHK Sci. & Tech. Res. Labs., 93, Ohmsha, Ltd, Tokyo (1995).
- [3] B. Javidi, F. Okano, "Three-Dimensional Television, Video, and Display Technologies," Springer, 4 (2002).
- [4] T. Ito, "Foundations of the 3D television", NHK Sci. & Tech. Res. Labs., 13, Ohmsha, Ltd, Tokyo (1995).
- [5] B. Lane, *Stereoscopic displays proceedings of the SPIE*, 0367 (1982).
- [6] T. Ito, "Foundations of the 3D television", NHK Sci. & Tech. Res. Labs., Ohmsha, Ltd, Tokyo, 135 (1995).
- [7] B. Javidi, F. Okano, "Three-Dimensional Television, Video, and Display Technologies", Springer, 35 (2002).
- [8] G. E. Favalora, R. K. Dorval, D. M. Hall, M. G. Giovinco, J. Napoli, "Volumetric 3D display system with rasterization hardware", *Proc. SPIE* 4297, 227 (2001).
- [9] A. Sullivan, "A Solid-state Multi-planar Volumetric Display", *SID'03*, 1531 (2003).
- [10] H. Takada, S. Suyama, K. Hiruma, and K. Nakazawa, "A Compact Depth-Fused 3-D LCD", *SID'03*, 1526 (2003).
- [11] G. K. Starkweather, "DSHARP- A Wide Screen Multi-projector Display", *SID'03*, 1535 (2003).
- [12] P. St. Hilaire, S. A. Benton, M. Lucente, P. M. Hubel, "Color Images with the MIT Holographic Video Display," *Proc. SPIE* 1667, 73 (1992).

- [13] Y. Kim, "Viewing-Angle-Enhanced 3-D Integral Imaging System Using a Curved Lens Array", *SID'04*, 1442 (2004).
- [14] B. Lee, S. Y Jung, J. H. Park, "Three-dimensional Integral Imaging Using LCD and LC Polarization Switcher", *Asian Symp. on Inf. Display*, 109 (2004).
- [15] H. Morishama, H. Nose, N. Taniguchi, K. Inoguchi, S. Matsumura, "A Eyeglass-Free Rear-Cross-Lenticular 3D Display", *SID Intl. Symp. Digest Tech. Papers* 29, 923-926 (1998).
- [16] D. J. Sandin, "Computer-generated Barrier-stripe Autostereography", *Proc. SPIE* 1083 (1989).
- [17] H. Isono, M. Yasuda, H. Sasazawa, "Autostereoscopic 3D LCD Display Using LCD-generated Parallax Barrier," in *Proc. 12th Int. Display Research Conf. '92*, 303 (1992).
- [18] K. W. Chien, H. P. D. Shieh, "Time-multiplexed 3D Displays based on Directional Backlights with Fast Switching Liquid Crystal Displays", *Appl. Opt.* 45, 3106 (2006).
- [19] Y. M. Chu, K. W. Chien, H. P. D. Shieh, J. M. Chang, A. Hu, Y. C. Shiu, V. Yang, "3D Mobile Display Based on Dual-Directional Light Guides with a Fast-Switching Liquid-Crystal Panel", *J. Soc. Inf. Display* 13, 875-879 (2005).
- [20] B. Javidi, F. Okano, "Three-Dimensional Television, Video, and Display Technologies," *Springer*, 36 (2002).
- [21] C. H. Chen, Y. C. Yeh, H. P. Shieh, J. M. Chang, A. Hu, V. Yang, Y. C. Shiu, C. L. Du, and S.C. Hsu, "Moiré Pattern and Image Crosstalk Reduction in 3-D Mobile Display," *SID'06 Digest*, 1154-1457 (2006).
- [22] A. Schmidt and A. Grasnick, "Multi-viewpoint Autostereoscopic Displays from 4D-vision," *Proc. SPIE* 4660, 212-221 (2002).
- [23] M. Halle, "Autostereoscopic Displays and Computer Graphics," *Computer Graphics, ACM SIGGRAPH* 31, 58-62 (1997).

- [24] J. Son, V. V. Saveljev, Y. Choi, J. Bahn, J. Kim, S. Kim, and B. Javidi, "Viewing Zones in Three-dimensional Imaging Systems Based on Lenticular, Parallax-barrier, and Microlens-array Plates," *Appl. Opt.* 43, 4985-4992 (2004).
- [25] J. Son, V. V. Saveljev, Y. Choi, J. Bahn, S. Kim, and H. Choi, "Parameters for Designing Autostereoscopic Imaging Systems Based on Lenticular, Parallax Barrier, and Integral Photography Plates," *Opt. Eng.* 42, 3326-3333 (2003).
- [26] L. Lipton and M. Feldman, "A New Autostereoscopic Display Technology: The SynthaGram™," *Proc. SPIE* 4660, 229-235 (2002).
- [27] "Sharp to Mass Produce World's First LCD to Simultaneously Display Different Information in Right and Left Viewing Directions," http://sharp-world.com/corporate/news/050714_2.html
- [28] G. Hamagishi, N. Sugiyama, S. Takemoto, Y. Tanaka, and T. Yata, "A Novel Double Display Screen with 2D and 3D Modes," *SID'06 Digest*, 1150-1153 (2006).
- [29] Y. Yeh and L. Silverstein, "Human Factors for Stereoscopic Color Displays," *SID'91 Digest*, 826-829 (1991).
- [30] G. Woodgate and J. Harrold, "A New Architecture for high Resolution Autostereoscopic 2D/3D Displays using Free-Standing Liquid Crystal Microlenses," *SID'05 Digest*, 378-381 (2005).
- [31] C. Berkel and J. Clarke, "Characterisation and Optimisation of 3D-LCD Module Design," *Proc. SPIE* 3012, 179-187 (1997).
- [32] C.H. Lai, C.H. Chen and H.P. D. Shieh, "A Novel 3D Double Screens Display," *IDW'06*, 1913-1916 (2006).
- [33] Paul May, "Reconfigurable 2D/3D Display," http://www.ocuity.co.uk/Ocuity_white_paper_Reconfigurable_2D-3D_Displays.pdf
- [34] I. Susumu, T. Nobuji and I. Morito, "Technique of stereoscopic image display," EP Pat. No. 0 354 851 (1990).

- [35] Y. Itoh, S. Fujiwara, N. Kimura, S. Mizushima, F. Funada, and M. Hijikigawa, *Proc. SID'98*, 221 (1998).
- [36] C. J. Wen, D. L. Ting, C. Y. Chen, L. S. Chuang, and C. C. Chang, *Proc. SID'97*, 1011 (1997).
- [37] K. Toyooka, T. Miyashita, T. Uchida, "The 3D Display Using Field-Sequential LCD with Light Direction Controlling Back-light", *SID'01*, 174 (2001).
- [38] T. Sasagawa, A. Yuuki, S. Tahata, O. Murakami, K. Oda, "Dual Directional Backlight for Stereoscopic LCD", *SID'03*, 399 (2003).
- [39] S. Ichinose, "Full-color Stereoscopic Video Pickup and Display Technique without Special Glasses", *Proc. SID'89*, 319 (1989).

